

Decreases in the excitability of motor axons contribute substantially to contraction fatigability
during neuromuscular electrical stimulation
by

Minh John Luu

A thesis submitted in partial fulfillment of the requirements for the degree of

Master of Science

Faculty of Physical Education and Recreation and Neuroscience

University of Alberta

© Minh John Luu, 2017

ABSTRACT

Activity-dependent changes in axonal excitability are well-documented, yet the contribution to contraction fatigability during neuromuscular electrical stimulation (NMES) is unclear. The present study was designed to: 1) characterize the magnitude and time course of changes in motor axon excitability before, during and after contractions produced at three stimulation frequencies, and 2) determine the relationship between changes at the axon, neuromuscular junction and muscle to the decline in torque observed at each frequency. Eight neurologically-intact participants attended three sessions during which NMES was delivered to the common peroneal nerve at 20, 40, or 60 Hz for 8 min (0.3 s “on”, 0.7 s “off”). Decreases in axonal excitability were measured as increases in current needed to produce an M-wave of 30% maximal (threshold current). Supramaximal stimuli were delivered over the nerve trunk or muscle belly to assess neuromuscular transmission and the force-generating capacity of the muscle, respectively. Torque decreased by 51 and 64% during 40 and 60 Hz NMES, respectively, but did not decrease significantly during 20 Hz NMES. The current required to produce the target M-wave increased 14, 27, and 35% during, and returned to baseline 1, 3, and 5 min following, 20, 40 and 60 Hz NMES, respectively. There was no other evidence of impaired neuromuscular transmission. Reduction in the force-generating capacity of the muscle was evident at 40 and 60 Hz NMES. Regression analysis showed decreases in torque were best predicted by decreases in axonal excitability overall, but were equally dependent on changes in the axon and muscle at each frequency. The present study demonstrates that activity-dependent decreases in axonal excitability contributes substantially to contraction fatigability during NMES.

PREFACE

This thesis is an original work by Minh John Luu. The research project described here has received approval from the University of Alberta Research Ethics Board, project name: “Does decreased excitability of the nerve under the stimulating electrodes contribute to “fatigue” of electrically-evoked contractions?”, No. Pro00060249, 31/08/2016.

ACKNOWLEDGEMENTS

My journey through a new city and degree could not have been done without the help of numerous individuals.

I would first like to express my deepest appreciation and gratitude towards Dr. David Collins who provided me an opportunity to work in his lab and whose constant guidance and mentorship have been invaluable throughout my MSc degree.

I would also like to express my sincerest gratitude towards my co-supervisor, Dr. Kelvin Jones, whose boundless knowledge and advice I could rely on for all aspects of research and life.

It is thanks to both Drs. Collins and Jones that I have grown as a researcher and whose teachings I will treasure and carry into future endeavours.

I would also like to thank both current and past members of the Human Neurophysiology Laboratory and Clinical and Theoretical Neuroscience Laboratory who have really made this journey enjoyable. From pilot studies to lunch time chats to lab outings, it's been amazing getting to know and work with each member.

I'd like to thank my MSc colleagues, Emily Ainsley and Francisca Claveria, who have struggled and succeeded on this journey with me from the start and whose companionship is irreplaceable.

A huge thank you must go to my girlfriend, Stephanie Nguyen, who has endured my selfish request for the past two years, and in return gave me endless encouragement, support and love.

Finally, a thank you goes to those from the ACElab who I've shared many great moments with.

TABLE OF CONTENTS

ABSTRACT	ii
PREFACE	iii
ACKNOWLEDGEMENTS	iv
CHAPTER 1: GENERAL INTRODUCTION	1
1.1 Overview	1
1.2 Neuromuscular Electrical Stimulation.....	2
1.3 Generating Contractions	5
1.4 Contraction Fatigability.....	10
1.5 Axonal Excitability.....	16
1.6 Thesis Outline.....	22
1.7 Figures	24
CHAPTER 2: DECREASES IN THE EXCITABILITY OF MOTOR AXONS CONTRIBUTE SUBSTANTIALLY TO CONTRACTION FATIGABILITY DURING NEUROMUSCULAR ELECTRICAL STIMULATION	27
2.1. Introduction	27
2.2. Methods	30
2.3. Results	38
2.4. Discussion.....	43
2.5. Figures	49
2.6. Tables.....	58
CHAPTER 3: GENERAL DISCUSSION	59
3.1. Contraction Fatigability.....	59
3.2. Safety Factors of Generating Contractions.....	61
3.3. Clinical Implications.....	62
3.4. Limitations.....	62
3.5. Future Directions	63
3.6. Summary.....	64
REFERENCES	65

LIST OF FIGURES

CHAPTER 1

Figure 1-1. Schematic of muscle activation – from motor unit recruitment to cross-bridge cycling. Figure is adapted from Westerblad, H., Lee, J. A., Lännergren, J., & Allen, D. G. (1991). Cellular mechanisms of fatigue in skeletal muscle. *American Journal of Physiology*, 261(30), C195–C209.

Figure 1-2. Distribution of channels across a myelinated axon. The axon is divided into the node, juxtaparanode and internode. *Inset:* Mechanism of action of membrane hyperpolarization in response to repetitive electrical stimulation.

Figure 1-3. Schematic diagram of threshold tracking. A stimulus response curve (center) is generated by progressively increasing current until the measured M-wave response reaches M_{\max} as shown on the left. The tracked M-wave amplitude of 30 % M_{\max} (threshold response) and associated current (threshold current) are indicated. Right diagram shows an example of modulating the current to maintain a steady 30 % M_{\max} response.

CHAPTER 2

Figure 2-1. Schematic description of the experimental protocol. Each session was comprised of three phases: *Pre-fatigue*, *Fatigue*, and *Post-fatigue*. The inset shows an expanded view of the first 20 s of the fatigue protocol, indicating the timing of threshold tracking and supramaximal pulses following each NMES train.

Figure 2-2. Electrode placement for nerve and muscle stimulation.

Figure 2-3. Representative data from a single participant at each of the three NMES frequencies.

A) The tracked M-waves (top) and torque generated by the NMES trains (bottom) during the *Fatigue* phase. Data show the superimposed traces ($n = 15$) from the first (left) and last (right) bin of the phase. The time course of changes in B) torque and C) threshold current elicited from NMES trains delivered at 20, 40 and 60 Hz during the *Fatigue* phase. Every 5th point is shown in (B) and (C) for clarity. Data from the *Pre-* and *Post-fatigue* phase showing D) overlaid M-waves during repetitive nerve stimulation, E) peak twitch torque and F) maximal voluntary contractions.

Figure 2-4. Binned A) train torque output, B) M_{\max} amplitude, and C) PTT during the fatigue protocol for each frequency. All data are expressed as mean \pm SD ($n = 8$). The open symbols indicate significant differences from the first bin across Time ($P < 0.05$). Asterisk (*) denotes when both 40 and 60 Hz groups are significantly different relative to 20 Hz ($P < 0.05$).

Figure 2-5. Binned threshold current normalized to the mean across the *Pre-fatigue* phase. All data are expressed as mean \pm SD ($n = 8$). The shaded area denotes the *Fatigue* phase. The open symbols denote significant increases from values recorded during the *Pre-fatigue* phase across Time ($P < 0.05$). Asterisks (*) denote significant timewise comparisons between frequencies as indicated by the pair of symbols ($P < 0.05$).

Figure 2-6. Mean (bold horizontal lines; $n = 8$) and individual participant (circles) data showing A) MVC and B) potentiated PTT before (empty circles) and after (filled circles) the fatigue protocol at each NMES frequency. The last pulse of the RNS test before (empty) and after (filled) the fatigue protocol are shown in (C). The dotted line represents a 10% decrement denoting a compromised NMJ. The 5th pulse of the RNS test is normalized to the 1st pulse. Asterisks (*) denote a significant decrease across Time ($P < 0.05$). Dagger (†) denotes a significant difference across Frequency ($P < 0.05$).

Figure 2-7. Linear regression relationship for torque evoked with A) 20 Hz ($R^2 = 0.17$, $P = 0.001$), B) 40 Hz ($R^2 = 0.72$, $P < 0.001$) and C) 60 Hz ($R^2 = 0.74$, $P < 0.001$), related to PTT and threshold current. Thick lines show the predicted torque based on the regression model. Solid circles with thin lines show the binned torque data. All data expressed as mean \pm SD ($n = 8$).

Figure 2-8. Beta coefficients for the relative predictive weights of threshold current (circle) and PTT (square) for each linear regression model. All data are expressed as $\beta \pm 95\%$ confidence intervals.

LIST OF TABLES

CHAPTER 2

Table 2-1. Multiple linear regression model for the effect of increases in threshold current and decreases in PTT on decreases in torque.

LIST OF ABBREVIATIONS

ANOVA	analysis of variance
ATP	adenosine triphosphate
CP	common peroneal
E-C	excitation-contraction
EMG	electromyography
EPP	end plate potential
FES	functional electrical stimulation
M_{max}	maximal M-wave amplitude
MU	motor unit
MVC	maximal voluntary contraction
M-wave	motor wave
NMES	neuromuscular electrical stimulation
NMJ	neuromuscular junction
NTF	neuromuscular transmission failure
PTT	peak twitch torque
rmANOVA	repeated measures analysis of variance
RNS	repetitive nerve stimulation
SCI	spinal cord injury
TA	tibialis anterior
TES	therapeutic/threshold electrical stimulation

CHAPTER 1: GENERAL INTRODUCTION

1.1 Overview

Neuromuscular electrical stimulation (NMES) is the application of an electric current to a nerve or muscle to elicit a muscular contraction. It can be used for rehabilitation in individuals with a motor impairment, such as a spinal cord injury (SCI) or stroke, by inducing contractions of paralyzed muscles (Bertoti, 2000; Peckham & Knutson, 2005; Sheffler & Chae, 2007). When incorporated into a rehabilitation program, NMES provides many therapeutic benefits to the user, counteracting some of the secondary complications that follow a motor impairment (Yarkony, Roth, Cybulski, & Jaeger, 1992). However, the efficacy of using NMES for rehabilitation is limited by the rapid onset and magnitude of contraction fatigability.

This thesis focuses on mechanisms that contribute to contraction fatigability during NMES. Contraction fatigability is defined as a decrease in torque following repeated contractions (Enoka & Duchateau, 2008; Kluger, Krupp, & Enoka, 2013). Past studies have attributed fatigability during NMES to impairments across the neuromuscular junction (NMJ) (B. Bigland-Ritchie, Jones, & Woods, 1979; Jones, Bigland-Ritchie, & Edwards, 1979; Sieck & Prakash, 1995) or within the contractile elements of the muscle (Edwards, Hill, Jones, & Merton, 1977; Jones, Howell, Roussos, & Edwards, 1982); however, there has been less attention on changes occurring within the axons. It is well known that the excitability of axons decreases following transmission of action potentials during both voluntary and electrically-evoked contractions (Kiernan, Lin, & Burke, 2004; Vagg, Mogyoros, Kiernan, & Burke, 1998). The excitability of an axon is defined by the inverse of the input required to just excite it (Burke, Kiernan, & Bostock, 2001), such that an increase in the required input implies a decrease in axonal excitability. Changes in axonal

excitability have been measured as a change in the intensity required of an external stimulus to depolarize an axon to threshold for action potential electrogenesis (Bergmans, 1970). The magnitude of changes in excitability has been found to be dependent on the level of activity in the axon such that there is a greater decrease in excitability following longer sustained voluntary contractions (Vagg et al., 1998) and higher stimulation frequencies (Kiernan et al., 2004). The study outlined in this thesis was designed to characterize the changes in axonal excitability when NMES is delivered at various stimulation frequencies. A secondary objective was to distinguish the extent to which changes at the axon, NMJ and muscle contribute to contraction fatigability during NMES. More specifically, the relative contribution of decreases in axonal excitability, neuromuscular transmission failure (NTF) and impairments in the force-generating capacity of the muscle were compared in predicting changes in torque output during NMES.

In the following sections I provide an overview of NMES, including its applications, benefits and limitations (§1.2). I then describe the similarities and differences between voluntary and electrically-evoked contractions (§1.3). In §1.4 I present literature outlining the current understanding of mechanisms contributing to fatigability during NMES. I introduce the concept of axonal excitability in §1.5, describing how it is measured and its application in research and clinical settings. Finally, §1.6 outlines the objectives of my thesis project.

1.2 Neuromuscular Electrical Stimulation

1.2.1 Applications

The term NMES typically refers to the excitation of intact peripheral nerves to elicit muscular contractions (Bertoti, 2000), but other terms may be used to describe specific applications of

NMES. Such terms include functional electrical stimulation (FES) and threshold or therapeutic electrical stimulation (TES). FES is the clinical application of NMES whereby muscles are stimulated in a coordinated manner to generate functional movement, with the intention of facilitating function for individuals with a motor impairment (Kralj & Bajd, 1989; Peckham & Knutson, 2005). Such functional movements include rowing (Taylor, Picard, & Widrick, 2011), standing (Jaeger, Yarkony, & Smith, 1989), walking (Kralj & Bajd, 1989) and cycling (Berkelmans, 2008). TES involves delivering low-level sub-contraction stimuli for relatively long periods, sometimes overnight, to promote blood flow to the muscle, theoretically strengthening muscle and reducing muscle atrophy and spasticity (K. Pape et al., 1993; K. E. Pape, 1997). However, a lack of evidence in support of these benefits and several randomized control trials have suggested that TES provides no significant improvements to either motor or ambulatory performance compared with a placebo (Dali et al., 2002; Fehlings, Kirsch, McComas, Chipman, & Campbell, 2002; Sommerfelt, Markestad, Berg, & Saetesdal, 2001). The focus of this thesis is on NMES in an experimental setting, with results extrapolated to improve FES as a rehabilitation tool for individuals with motor impairments following a neurological disease or injury (Knutson, Fu, Sheffler, & Chae, 2015; Sheffler & Chae, 2007).

1.2.2 History

The first use of electricity as a therapeutic intervention dates as far back as 2750 BC to ancient Egypt, where Nile catfish were used for pain relief (Heidland et al., 2013). The first documented individual to be cured with electrical stimulation was a Roman slave during the time of Emperor Tiberius Caesar who mistakenly stepped on an electric ray, consequently relieving his pain from gout (Cambridge, 1977). Following this, other documented evidence emerged of Greek and Roman

use of the electric ray for pain relief, gout and arthritis circa 40 AD (Cambridge, 1977; Heidland et al., 2013; Macdonald, 1993). The wide-spread use of electricity for rehabilitation was not until hundreds of years later, following the invention of the Leyden jar – considered the first capacitor – in the 18th century (Stillings, 1983).

The birth of electrophysiology came with Luigi Galvani's discovery that an electric current applied to the muscles of severed frog legs generates a contraction (Heidland et al., 2013; Macdonald, 1993; Schechter, 1971). In the late 1700s, Giovanni Aldini extended Galvani's findings from animals to human cadavers, promoting electrical stimulation as a therapeutic tool (Parent, 2004). At the turn of the century, electrical stimulation became recognized as a potential treatment in individuals with various mental disorders. In the late 19th century, Duchenne developed surface electrodes used to localize stimulation and in 1961, the first functional use of electrical stimulation was packaged in a foot drop stimulator for hemiplegic patients (Liberson, Holmquest, Scot, & Dow, 1961). Since then, research has greatly advanced on the use of NMES for both upper- and lower-limb orthotics and for rehabilitation in individuals with various motor impairments (Kralj & Bajd, 1989; Sheffler & Chae, 2007).

1.2.3 Benefits and Limitations

NMES provides numerous benefits, particularly in individuals experiencing paralysis who rely on NMES to generate contractions (Hamzaid & Davis, 2009). For example, in individuals with a SCI, FES cycling 3 times per week can increase total and lower limb lean body mass (Baldi, Jackson, Moraille, & Mysiw, 1998), bone mineral density (Frotzler et al., 2008) and resistance to contraction fatigability (Cramer, Weston, Climstein, Davis, & Sutton, 2002). Other benefits of

NMES have included reductions in spasticity (Yan, Hui-Chan, & Li, 2005), increases in maximal torque output and peak power (Duffell et al., 2008) and improved range of motion (Bajd, Kralj, Turk, Benko, & Segal, 1989; Yan et al., 2005) and cardiovascular fitness (Wheeler et al., 2002).

Despite the many benefits NMES provides, it is still limited as a rehabilitation tool because of the discomfort associated with the stimulation and the rapid development of contraction fatigability (Maffiuletti, 2010; R. Martin, Sadowsky, Obst, Meyer, & McDonald, 2012). In order to maintain force output, the stimulus amplitude is progressively increased, resulting in increased user discomfort (Broderick, Kennedy, Breen, Kearns, & Ólaighin, 2011). The user's tolerability to the stimulus would therefore limit the maximum force achieved and the number of evoked contractions, thus decreasing the intensity and duration of the given task. The need to increase stimulus amplitude to maintain force output, however, can be considered a consequence of the rapid development and magnitude of contraction fatigability which further limits the number and intensity of evoked contractions. Therefore the purpose of this thesis is to explore mechanisms contributing to contraction fatigability during NMES.

1.3 Generating Contractions

The first step in investigating contraction fatigability is to understand how contractions are generated. The control and activation of a muscle is driven by the collective activation of motor unit (MU) populations; each MU defined as an alpha motoneuron and the muscle fibres it innervates. The following sections provide an overview of how contractions are generated and a detailed description of MU behaviour during both voluntary and electrically-evoked contractions.

In this thesis, I limit the scope of how contractions are generated to peripheral elements that are common to both voluntary and electrically-evoked contractions, as illustrated in Figure 1-1.

The first element shared by both voluntary and electrically-evoked contractions is the depolarization of motor axons (a). This depolarization is achieved via excitatory post synaptic potentials at the cell body during voluntary contractions or an induced change in transmembrane potential along the axon during electrically-evoked contractions (Hakan Westerblad, Lee, Lännergren, & Allen, 1991). Though it is possible to electrically-evoke a contraction through direct activation of the muscle membrane, the stimulus amplitude required is substantially larger than that required to activate the axon (Mortimer, 2011). Therefore, contractions are commonly generated through the depolarization of the nerve and not the muscle during NMES. If there is a sufficient change in the transmembrane potential, either at the cell body or along the axon, such that voltage-gated sodium channels switch to an activated state, an action potential is initiated. The action potential then propagates down the length of the axon (b) to the terminal branches. When the action potential depolarizes the axon terminals, calcium channels open and the resulting influx of calcium causes the release of acetylcholine into the NMJ. Acetylcholine then binds to nicotinic acetylcholine receptors on the post-synaptic cleft (c), thereby opening those channels, permitting a sodium influx to depolarize the muscle membrane. Action potentials then transmit along the sarcolemma (d) and down the transverse tubules (e). The change in voltage triggers activation of voltage-sensing dihydropyridine receptors along the transverse tubules, which open adjacent ryanodine receptors on the sarcoplasmic reticulum. This results in the release of calcium ions from the sarcoplasmic reticulum (f). Free calcium ions within the myoplasm bind to troponin C causing a shift in tropomyosin. This exposes the binding sites of actin to myosin for cross-bridge cycling

(g) and enables the muscle to contract (h). Subsequent muscle relaxation occurs when ATP-dependent calcium pumps move calcium ions from the myoplasm back into the sarcoplasmic reticulum (i). Though this process is common to both voluntary and electrically-evoked contractions, differences in the way MUs are recruited and discharge between the two types of contractions increase the susceptibility of electrically-evoked contractions to fatigability.

1.3.1 Voluntary Contractions

During a voluntary contraction, synaptic input aggregated from supraspinal centres and sensory receptors drive the activation of MUs. MUs are recruited in an orderly fashion with increasing synaptic input according to the size of the motoneuron's cell body (Henneman, Somjen, & Carpenter, 1965). According to Henneman's size principle, during a voluntary contraction, small motoneurons which innervate fatigue-resistant muscle fibres are recruited first, proceeded by larger motoneurons which innervate muscle fibres more susceptible to fatigue (Milner-Brown, Stein, & Yemm, 1973). This recruitment order allows weak contractions to be sustained for long periods and reduces the rate of contraction fatigability.

During voluntary contractions, MUs are recruited asynchronously with respect to each other at low discharge frequencies, minimizing the metabolic demand placed on an individual MU. MUs typically discharge at frequencies less than 10 Hz during recruitment (De Luca & Contessa, 2012), and exhibit variable discharge frequencies depending on the contractile speed, strength and the muscle. At the onset of a rapid contraction, MUs can achieve instantaneous discharge frequencies as high as 120 Hz in the tibialis anterior (TA) muscle (Desmedt & Godaux, 1977), while mean discharge frequencies between 15 to 23 Hz are observed during a contraction at 50% the strength

of a maximal voluntary contraction (MVC), and up to 30 Hz during a contraction at 75% of MVC (B. R. Bigland-Ritchie, Furbush, Gandevia, & Thomas, 1992; Connelly, Rice, Roos, & Vandervoort, 1999). The importance of modulating MU discharge frequencies as a means to increase contraction strength has been recently highlighted in a review (Enoka & Duchateau, 2017), suggesting approximately 75% of the torque generated during an MVC is due to increases in discharge frequencies of individual MUs.

1.3.2 Electrically-Evoked Contractions

In contrast to voluntarily driving MU activity through descending synaptic inputs, NMES depolarizes the axons of a peripheral mixed nerve to generate a contraction. This type of MU activation results in a random MU recruitment order which increases the susceptibility of electrically-evoked contractions to fatigability.

At rest, the uneven distribution of ions across the axonal membrane results in a net negative membrane potential relative to the surrounding extracellular fluid (Hille, 2001). During NMES, a pair of electrodes, consisting of a negative (cathode) and a positive electrode (anode), influence the flow of ions in the tissue beneath them to generate an electric potential. Depolarization occurs below the cathode as negatively charged ions in the extracellular space are repelled from the electrode towards the membrane, while positively charged ions aggregate below the membrane due to the attractive pull of the cathode. This results in a decrease in the potential difference between the inside and outside of the axon membrane and a depolarization of the membrane potential. In contrast, the reverse occurs below the anode, with negatively charged ions accumulating intracellularly while positively charged ions accumulate extracellularly. This results

in an increase in the potential difference across the axon membrane, i.e. membrane hyperpolarization.

During electrically-evoked contractions, MU recruitment order diverges from the size-ordered recruitment observed during voluntary contractions. A combination of axon diameter and proximity to the stimulating electrodes determines which MU will be recruited (Bickel, Gregory, & Dean, 2011). Large axons depolarize before small axons due to reduced axial resistance, while MUs closer in proximity to the surface electrodes are exposed to a stronger electric field. This results in a random recruitment of MUs, with respect to type (Bickel et al., 2011). Accordingly, this leads to an increased number of fast glycolytic muscle fibres contributing to contractions during NMES compared to during voluntary contractions of similar strength.

Another factor which further increases the susceptibility of NMES-evoked contractions to fatigability is the relatively high MU discharge frequencies. During NMES, MUs discharge synchronously with the stimulus pulse, therefore their discharge frequency is governed by the stimulation frequency. Typically, frequencies employed in the clinic range between 20 to 60 Hz (Berkelmans, 2008) to generate fused contractions (Jaeger et al., 1989) of sufficient amplitude for the task. These frequencies are substantially higher than discharge frequencies during voluntary contractions of similar strength, increasing the metabolic demand on the muscle (Hakan Westerblad et al., 1991). A cross-comparison of stimulation frequencies, pulse widths, and intensities used during NMES revealed that high stimulation frequencies were the biggest contributor to fatigability (Behringer et al., 2016; Gorgey, Black, Elder, & Dudley, 2009).

Therefore, the focus of this thesis will be on mechanisms contributing to contraction fatigability across a range of NMES frequencies used in the clinic.

1.4 Contraction Fatigability

Contraction fatigability is a multifactorial phenomenon with underlying mechanisms influenced by the task performed (Enoka & Duchateau, 2008). During NMES, fatigability can develop due to failure at any site along the pathway described in Figure 1-1. Traditionally, fatigability has been attributed to impairment of neuromuscular transmission and/or a breakdown in excitation-contraction coupling (E-C coupling) (Edwards, 1984; Jones, 1996). For clarity in this thesis, I define neuromuscular transmission to include elements proximal to the transverse tubules, i.e. action potential propagation along the axon, release of acetylcholine from the pre-synaptic cleft, depolarization of the muscle membrane, and action potential propagation along the muscle surface (Figure 1-1(a) – (d)) (Sieck & Prakash, 1995). On the other hand, E-C coupling encompasses all mechanisms distal to and including the transverse tubules, i.e. signal transmission from the transverse tubules to the sarcoplasmic reticulum, calcium release and re-uptake from the myoplasm, and activation of cross-bridge cycling (Figure 1-1(e) – (i)) (Dulhunty, 2006; Stephenson, Lamb, Stephenson, & Fryer, 1995).

1.4.1 Neuromuscular Transmission

Previous studies have attributed NTF to originate at the NMJ (Sieck & Prakash, 1995) or along the muscle membrane (B. Bigland-Ritchie et al., 1979). NTF can result from a depletion in neurotransmitter stores (Sieck & Prakash, 1995) but in humans (Wood & Slater, 2001), it has primarily been attributed to changes in the ion distribution along the muscle membrane resulting

in action potential propagation failure (Edwards, 1984; Jones et al., 1979). Following the propagation of an action potential along the sarcolemma, there is a net increase in extracellular potassium and intracellular sodium (Allen, Lamb, & Westerblad, 2008; Juel, 1986; Mckenna, Bangsbo, & Renaud, 2008). Although the sodium-potassium pump may restore the concentration gradient, repetitive activity will change the ion distribution across the membrane (Hakan Westerblad et al., 1991). This shift in ion concentration reduces the muscle membrane potential (Juel, 1986), resulting in inactivation of voltage-gated sodium channels, and reductions in action potential amplitude. These transient changes in ion concentrations are suggested to contribute to the transient force loss and rapid recovery associated with fatigability due to NTF (Jones et al., 1979).

Tests used to detect NTF include comparing the rates of fatigability between nerve and muscle stimulation (Aldrich, Shander, Chaudhry, & Nagashima, 1986), and analyzing changes in the end plate potentials (EPPs) (Krnjevic & Miledi, 1958) or maximal motor wave (M_{max}) (Brenda Bigland-Ritchie, Kukulka, Lippold, & Woods, 1982). Early evidence in support of NTF was found using an isolated rat phrenic nerve-diaphragm preparation (Aldrich et al., 1986; Krnjevic & Miledi, 1958, 1959; Thesleff, 1959). In a study comparing direct stimulation of the diaphragm muscle (using *d*-tubocurarine to prevent activation of terminal branches), and indirect stimulation of the muscle via the phrenic nerve, investigators found force was more attenuated following stimulation via the nerve than the muscle (Aldrich et al., 1986). This finding led the authors to conclude that fatigability occurred predominantly proximal the muscle.

Other studies have utilized changes in the EPPs to investigate NTF (Sieck & Prakash, 1995). Following 50 Hz stimulation for 5 min *in vitro*, there was an increase in intermittent failures in the EPP attributed to a conduction block along the axon's terminal branches during continuous stimulation of the phrenic nerve (Krnjevic & Miledi, 1958, 1959). In addition, the incidence of failure increased with higher stimulation frequencies (Krnjevic & Miledi, 1959). On the other hand, Thesleff (1959) attributed reductions in successive evoked EPPs following 150 ms at 20 Hz to a decrease in neurotransmitter release, evidenced when infusion of acetylcholine generated constant amplitude EPPs. However, at frequencies above 60 Hz, infusion of acetylcholine evoked no response, suggesting that at higher frequencies, there may be a desensitization of the motor endplate to acetylcholine, which was found to last approximately 0.2 s (Thesleff, 1959). Despite these findings in the rat, it has been argued that in humans, the inherent safety factor across the NMJ prevents such failures from occurring even during extreme movements (Wood & Slater, 2001), while a 5:1 safety margin at the nodes of Ranvier ensures reliable action potential propagation (Tasaki, 1953).

Decreases in M_{\max} amplitude have also been used to test for NTF during a variety of tasks. These include maximal (Stephens & Taylor, 1972; C K Thomas, Woods, & Bigland-Ritchie, 1989) and submaximal (Fuglevand, Zackowski, Huey, & Enoka, 1993) voluntary contractions of the first dorsal interosseous muscle, and following supramaximal stimulation of the ulnar and peroneal nerves (Milner-Brown & Miller, 1986). Despite this evidence, other studies have found no change in M_{\max} when maximally contracting the adductor pollicis (Brenda Bigland-Ritchie et al., 1982; Merton, 1954), TA (C K Thomas et al., 1989), during short MVCs of the first dorsal interosseous muscle (Brenda Bigland-Ritchie et al., 1982), and following stimulation of the diaphragm muscle

(Roussos & Aubier, 1981). The reasons for these discrepancies is currently unclear but this has led to controversial conclusions that fatigability is primarily attributed to distal failure within the contractile elements of the muscle. In this thesis, measures of M_{max} are regularly taken to assess for neuromuscular transmission and propagation along the muscle membrane, while repetitive nerve stimulation (RNS) is utilized to specifically assess transmission across the NMJ.

Repetitive stimulation of the motor nerve, sometimes known as the Jolly test, is one of the most commonly used clinical tools to assess transmission across the NMJ (Chiou-Tan et al., 2001; Costa, Evangelista, Conceição, & de Carvalho, 2004; Rich, 2006). Another electrodiagnostic tool to assess NMJ transmission is single fibre EMG, sometimes known as the jitter test (Rich, 2006). Comparing these tests, the jitter test provides a more sensitive clinical measure of NTF but is less commonly used due to the invasiveness and technical difficulty of this test. The jitter test involves using fine wire to record EMG from two muscle fibres of the same MU. The MU is then repetitively activated either voluntarily or electrically, and variation in the latencies of the response at each muscle fibre is compared. Low variation indicates similar latencies between the two muscle fibres and is indicative of healthy neuromuscular transmission (Rich, 2006; Chiou-Tan et al, 2001).

Clinically, RNS is more commonly used due to the non-invasive nature of the test, and technical simplicity. This test involves measuring the M-wave amplitude in response to a train of 5 to 10 supramaximal stimuli delivered to the nerve trunk at frequencies between 2 to 5 Hz (Chiou-Tan et al., 2001; Ozdemir & Young, 1976). Progressive reduction across the train of M-waves is indicative of presynaptic impairments as assessed in individuals with myasthenia gravis, while potentiation of the M-waves is indicative of post-synaptic impairments as assessed in individuals

with Lambert-Eaton syndrome (Chiou-Tan et al., 2001; Zivković & Shipe, 2005). Though this test is less sensitive than the jitter test, it is still widely used as a first-line diagnosis tool of impaired neuromuscular transmission with an approximated 80% sensitivity rating when tested in individuals diagnosed with myasthenia gravis for longer than four weeks (Liik & Punga, 2016). In this thesis, RNS testing using five supramaximal pulses delivered at 3 Hz is performed before and after a fatigue protocol to test for compromised transmission across the NMJ.

1.4.2 Excitation-Contraction Coupling

Fatigability has been attributed to failure occurring in the contractile elements of the muscle when no measurable change in neuromuscular transmission was observed (Brenda Bigland-Ritchie et al., 1982; Merton, 1954; Merton, Hill, & Morton, 1981; C K Thomas et al., 1989). A breakdown in E-C coupling can result from decreases in calcium release or re-uptake from the myoplasm, and/or reduced calcium sensitivity or activation of cross-bridge cycling (Jones, 1996; Keeton & Binder-Macleod, 2006). Edwards et al (1977) noted a long-lasting depression in torque following both repeated voluntary and electrically-evoked contractions that could not be attributed to changes in ATP and creatine phosphate levels, muscle membrane excitation nor action potential propagation, suggesting the fault occurred in the muscle's contractile mechanisms.

E-C coupling has been studied and assessed through single muscle fibre preparations (H Westerblad, Duty, & Allen, 1993), comparing measures of peak twitch torque (PTT) and M_{max} (Place, Yamada, Bruton, & Westerblad, 2010), and comparing tetanic torque elicited with low and high stimulation frequencies before and after a fatiguing task (Binder-Macleod & Russ, 1999; Edwards, Hill, et al., 1977; Edwards, Young, Hosking, & Jones, 1977; A. Martin et al., 2016).

Evidence in support of reductions in calcium release or sensitivity were found in mouse and human muscle preparations, when exposure to low dosages of caffeine, a promoter of calcium release from the sarcoplasmic reticulum (Endo, 1975), reversed fatigability following 3 min stimulation alternating 30 and 100 Hz trains (Jones et al., 1982). Later studies corroborated these findings of reduced calcium release from the sarcoplasmic reticulum as a contributor to fatigability following intermittent stimulation until force declined to 30% in single muscle fibre preparations (H Westerblad et al., 1993). However, excessive increases in myoplasmic calcium may lead to a breakdown in E-C coupling through activation of calcium-dependent proteases (Lamb, 2009). Changes in metabolite concentrations, such as reductions in glycogen stores, increases in magnesium and hydrogen ion concentrations, and accumulation of inorganic phosphate, lactate, and reactive oxygen species, have also been linked to contraction fatigability (Allen et al., 2008; Fitts, 1994; Håkan Westerblad, Allen, & Lännergren, 2002; Hakan Westerblad et al., 1991). The increased lactate and hydrogen ion concentrations can also lead to decreases in pH of the blood, resulting in complete inhibition of phosphorylase and phosphofructokinase – enzymes involved in glycolysis (Hermansen, 1981). This reduces ATP re-synthesis and leads to a negative impact on the calcium sensitivity and contractile capacity of the muscle (Hermansen, 1981).

In the present study, we evaluated the E-C coupling mechanism using single supramaximal stimuli delivered over the TA muscle belly and measured the resultant PTT. We opted to stimulate over the muscle belly rather than the nerve trunk because of the different muscles the common peroneal (CP) nerve supplies. The CP nerve can be divided into superficial and deep branches. The superficial branches innervate peroneus brevis and peroneus longus, which produce ankle eversion, while the deep peroneal branch innervates tibialis anterior, extensor hallucis and extensor

digitorum longus, producing ankle dorsiflexion. Therefore, stimulation over the muscle belly minimizes contributions of these other muscles to the PTT.

1.5 Axonal Excitability

Though there have been many studies examining fatigability during NMES, the notion of changes in axonal excitability being a contributing mechanism has often been overlooked. In past studies investigating mechanisms contributing to fatigability, supramaximal stimulation is typically employed to ensure full activation of the nerve (Edwards, Hill, et al., 1977; Jones et al., 1979). Similarly, in the clinic, stimulus intensity is progressively increased to maintain cycling cadence and power, inadvertently combating reduced axonal excitation. Despite the frequent use of supraliminal stimulus intensities, fatigability during NMES is attributed to mechanisms distal to and including the NMJ. An objective of this thesis is to therefore determine whether fatigability during NMES is, in part, attributed to reductions in axonal excitability, leading to decreased recruitment of muscle fibres contributing to the torque.

Recently, evidence has emerged suggesting that reduced axonal excitability contributes to contraction fatigability during NMES (Matkowski, Lepers, & Martin, 2015; Papaiordanidou, Stevenot, Mustacchi, Vanoncini, & Martin, 2014). Papaiordanidou et al. (2014) found that tetanic torque decreased faster when elicited with 100 Hz compared to 30 Hz NMES at submaximal intensities, and that the decrease was greater than changes in twitch torque evoked with single stimuli at supramaximal intensities. The authors suggested that decreases in the excitability of the innervating axons lead to this discrepancy. Matkowski et al. (2015) corroborated these findings using supramaximal stimuli interlaid in the middle of trains of submaximal stimuli. The authors

demonstrated that these superimposed stimuli evoked a twitch torque which decreased slower than the torque produced with the tetanic stimulation (Matkowski et al., 2015).

1.5.1 Types of Channels on a Myelinated Axon

The excitability of an axon is a function of both the density and activity of its ion channels. Figure 1-2 shows the organization of these ion channels along the axon membrane, highlighting where the density of each channel is highest. In the myelinated axon, channels are distributed in three main regions: the node, the juxtaparanode, and the internode (Burke et al., 2001). The highest concentration of voltage-gated sodium channels resides within the node, approximately 30-fold higher in density than at the internode (Burke et al., 2001; Waxman & Ritchie, 1985). In contrast, voltage-gated potassium channels are in high concentration below the myelin sheath at the juxtaparanode and internode, while in lower concentrations at the node (Burke et al., 2001; Waxman & Ritchie, 1985). These differences result in action potential electrogenesis at the node, leaving the internodal membrane electrically inexcitable, and generating the saltatory conduction observed in myelinated axons. Within the node, there is also a high density of persistent sodium channels and slow-kinetic potassium channels relative to other regions. These channels activate in response to a membrane depolarization, but have opposing functions. Persistent sodium channels activate at potentials 10-20 mV negative that of transient sodium channels and act to slowly depolarize the membrane (Bostock & Rothwell, 1997); whereas slow-kinetic potassium channels accommodate to depolarizing stimuli by hyperpolarizing the membrane. A similar accommodative function is served by inward rectifying channels in the internode which depolarize the membrane through the influx of cations (both sodium and potassium ions) in response to hyperpolarizing stimuli. This hyperpolarization-activated cation conductance has been regularly termed I_H (Burke

et al., 2001). The final component contributing to the excitability of the axon is the sodium-potassium pump, which activates in response to an accumulation of intracellular sodium ions, transporting a net positive charge extracellularly (De Weer & Geduldig, 1973). Taken together, the resting membrane potential is therefore determined by a combination of the sodium-potassium pump, persistent sodium channels, and slow-kinetic potassium channels.

1.5.2 Differences Between Axons

Motor axons innervating slow-twitch muscle fibres express greater I_H activity compared with those innervating fast-twitch fibres as found in a rat model (Lorenz & Jones, 2014). A suggested reason for this difference was that the slow-twitch muscle fibres would tend to hyperpolarize more due to higher levels of daily activity and that this adaptation offsets the increased levels of hyperpolarization. Similarly, a comparison between motor and sensory axons found sensory axons to have higher I_H activity than motor axons (Howells, Trevillion, Bostock, & Burke, 2012), and also have a greater density of persistent sodium channels relative to motor axons (Bostock & Rothwell, 1997). The greater density of persistent sodium channels results in a longer strength-duration time constant and lower rheobasic current, enabling the preferential activation of sensory axons relative to motor when using low-intensity, wide-pulse stimuli during NMES (Bostock & Rothwell, 1997; Panizza et al., 1998; Veale, Mark, & Rees, 1973).

1.5.3 Measuring Axonal Excitability

Current clinical assessments of peripheral nerve function are performed using nerve conduction studies, however, results of such a test provide limited information and lack insight into the biophysical changes contributing to an altered M-wave latency. A series of tests to assess axonal

excitability have been developed by Dr. Hugh Bostock (Bostock, Cikurel, & Burke, 1998), and rely on a technique called “threshold-tracking” (Bergmans, 1970). The basis of this technique relies on repeatedly measuring the amount of current required to just elicit a target or “threshold” M-wave amplitude to infer changes in axonal excitability (Figure 1-3). Thus, decreases in axonal excitability can be inferred from increases in the current. Typically, target amplitudes are set at 30 – 50% M_{\max} as it lies along the steepest part of a stimulus-response curve providing the most sensitivity (small changes in current causing large changes in M-wave amplitude). The target M-wave amplitude is denoted as the “threshold response,” while the current to elicit this response is the “threshold current.”

Many studies have demonstrated that changes in the threshold current can provide insight into the ionic and biophysical properties of axons (Burke et al., 2001; Krishnan, Lin, Park, & Kiernan, 2009; Nodera & Kaji, 2006); therefore, many investigators have utilized this technique to examine excitability changes in motor and sensory axons to better understand the pathophysiology of a number of neural disorders (Krishnan et al., 2009). Examples of neural disorders investigated include individuals with diabetic neuropathies (Krishnan, Lin, & Kiernan, 2008), cerebral palsy (Klein, Zhou, & Marciniak, 2015), amyotrophic lateral sclerosis (Vucic, Krishnan, & Kiernan, 2007), and a SCI (Lin et al., 2007).

Using a simplified version of this threshold-tracking technique, investigators have also studied the extent to which changes in axonal excitability can occur following voluntary (Kuwabara, Cappelen-Smith, Lin, Mogyoros, & Burke, 2002; Vagg et al., 1998) and electrically-evoked contractions (Kiernan et al., 2004). Authors reported increases in the threshold current suggesting

a decrease in excitability caused by axonal membrane hyperpolarization (Bostock & Grafe, 1985). Furthermore, the magnitude of change was dependent on the impulse load, i.e. discharge frequency and duration. Vagg et al. (1998) showed that the increase in threshold current was greater and had a longer time course for recovery following a 60 s MVC of the thumb abductors when compared to a 15 s MVC. A similar activity-dependent pattern was found following stimulation of the digital nerves (Vagg et al., 1998) and median nerve (Kiernan et al., 2004), with higher stimulation frequencies inducing greater increases in threshold current followed by longer recovery times compared with stimulation at lower frequencies. The present project utilizes threshold tracking to measure the magnitude and time course of changes in motor axon excitability during NMES across various stimulation frequencies.

1.5.4 *M-waves*

Changes in the parameters of the EMG signal have previously been used as an indicator of muscle fatigability (Merletti, Lo Conte, & Orizio, 1991). During voluntary contractions, calculations of the average rectified value and the root mean square can be used as a representation of the amplitude of surface EMG, with decreases suggesting fatigability. Declines in the conduction velocity along the axon or at the muscle membrane can also be inferred from a decrease in the mean or median frequency of the EMG's power spectrum (Merletti et al., 1991). During electrically-evoked contractions, the M-wave can be used as an indicator of neuromuscular fatigue and axonal activation. The submaximal M-wave and M_{\max} are representative of the excitation of a subset of axons or an entire motor pool, respectively. As such, changes in the M-wave can be indicative of changes in the properties of that subset of axons (Bostock et al., 1998), while decreases in M_{\max} have been used as an indicator of NTF (Fuglevand et al., 1993). However, it

should be acknowledged that aside from reduced axonal excitability causing drop out of MUs, other factors may also contribute to changes in the M-wave amplitude (Keenan, Farina, Merletti, & Enoka, 2006).

Joint position has been demonstrated to influence M_{\max} amplitude (Frigon, Carroll, Jones, Zehr, & Collins, 2007; Tucker & Turker, 2007). Changes in the joint position alter the level of muscle bulk below the recording electrodes which in turn affects the M_{\max} amplitude (Frigon et al., 2007). With the ankle dorsiflexed, M_{\max} measured in the TA was larger, while M_{\max} in the soleus was larger during ankle plantarflexion (Frigon et al., 2007). Physiological changes that can affect the M-wave, apart from the number of axons, are changes in MU properties (Keenan et al., 2006), the ionic distribution across the muscle membrane (Hicks & McComas, 1989; Jones, 1981), or the ratio of inactivated sodium channels (Choi, Hudmon, Waxman, & Dib-Hajj, 2006). A comparison of parameters that may influence the M-wave shape was modelled using a computer simulation based on known physiological properties of the first dorsal interosseous muscle (Keenan et al., 2006). These parameters included decreasing the number of activated MUs resulting in declines in M_{\max} amplitude, decreasing MU conduction velocity increasing the delay and dispersion of the waveform, and decreasing the shape of the intracellular action potential resulting in a combination of amplitude decreases and waveform delay and dispersion (Keenan et al., 2006). Whereas increases in M_{\max} have also been observed and attributed to either enlargement of the intracellular action potential amplitude (Hicks & McComas, 1989) or more effective summation of the individual intracellular potentials (Cupido, Galea, & McComas, 1996). Hicks and McComas (1989) noted a hyperpolarization of the muscle membrane following repetitive stimulation of the rat soleus *in situ*, attributed to increased activity of the sodium-potassium pump leading to larger

potentials. Others that have examined changes in the ion concentration across the membrane noted increased extracellular potassium and intracellular sodium (Nagaoka, Yamashita, Mizuno, & Akaike, 1994). While the increase in extracellular potassium is suggested to slow action potential propagation reducing M-wave amplitude (Jones, 1981), others attribute the build up of intracellular sodium and reductions in extracellular sodium within the transverse tubules leads to reduced action potential amplitude and if sufficiently depressed, result in action potential propagation failure (Allen et al., 2008; Bezanilla, Caputo, Gonzalez-Serratos, & Venosa, 1972).

1.6 Thesis Outline

It is known that the excitability of active axons decreases following both voluntary and electrically evoked contractions; however, only recently has the contribution of decreases in axonal excitability to contraction fatigability during NMES been investigated experimentally. The present thesis was designed to address two primary questions: 1) What is the magnitude and time course of changes in axonal excitability during three frequencies of NMES? and 2) To what extent do changes in the axon, NMJ and muscle contribute to contraction fatigability at each of the observed NMES frequencies. Specifically, we aim to determine the relationship between declines in torque and changes in axonal excitability, transmission across the NMJ and the force-generating capacity of the muscle.

In this experiment, NMES was delivered at 20, 40 and 60 Hz which encapsulates the range of stimulation frequencies employed in the clinic (Berkelmans, 2008; de Kroon, IJzerman, Chae, Lankhorst, & Zilvold, 2005). I hypothesize that decreases in axonal excitability play a role in contraction fatigability induced at each of these frequencies, and that the magnitude of change will

be larger, onset will be sooner and the time course of recovery will be longer with higher NMES frequencies. Furthermore, the relative contribution to fatigability of this frequency-dependent decrease in axonal excitability will be greater at higher NMES frequencies. I also hypothesize that NTF and the breakdown in E-C coupling will contribute less to fatigability.

1.7 Figures

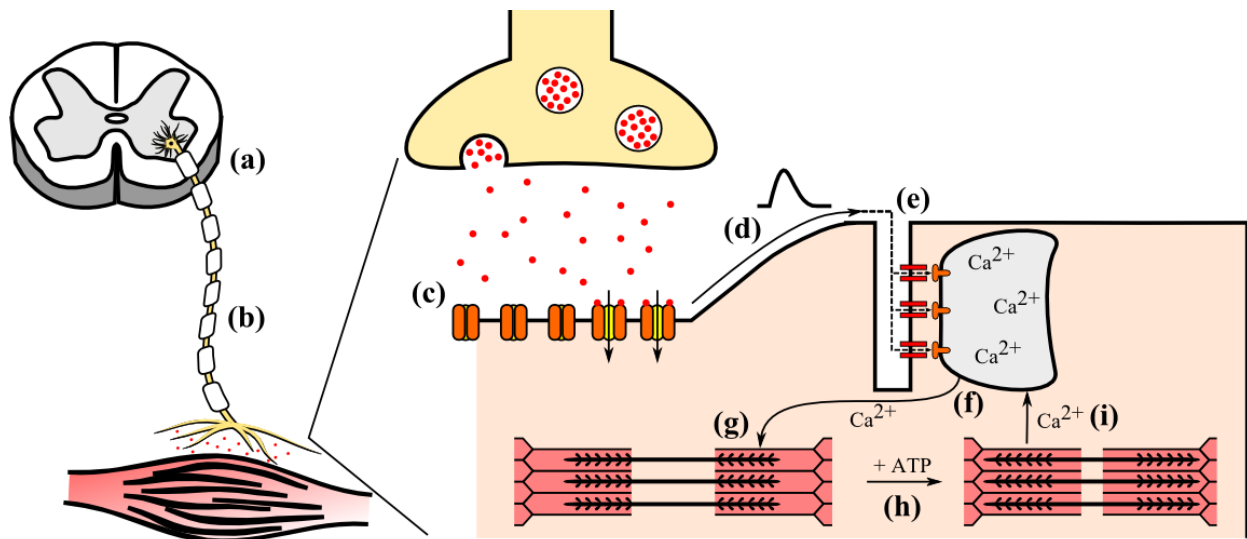


Figure 1-1. Schematic of muscle activation – from motor unit recruitment to cross-bridge cycling.

Figure is adapted from Westerblad, H., Lee, J. A., Lännergren, J., & Allen, D. G. (1991). Cellular mechanisms of fatigue in skeletal muscle. *American Journal of Physiology*, 261(30), C195–C209.

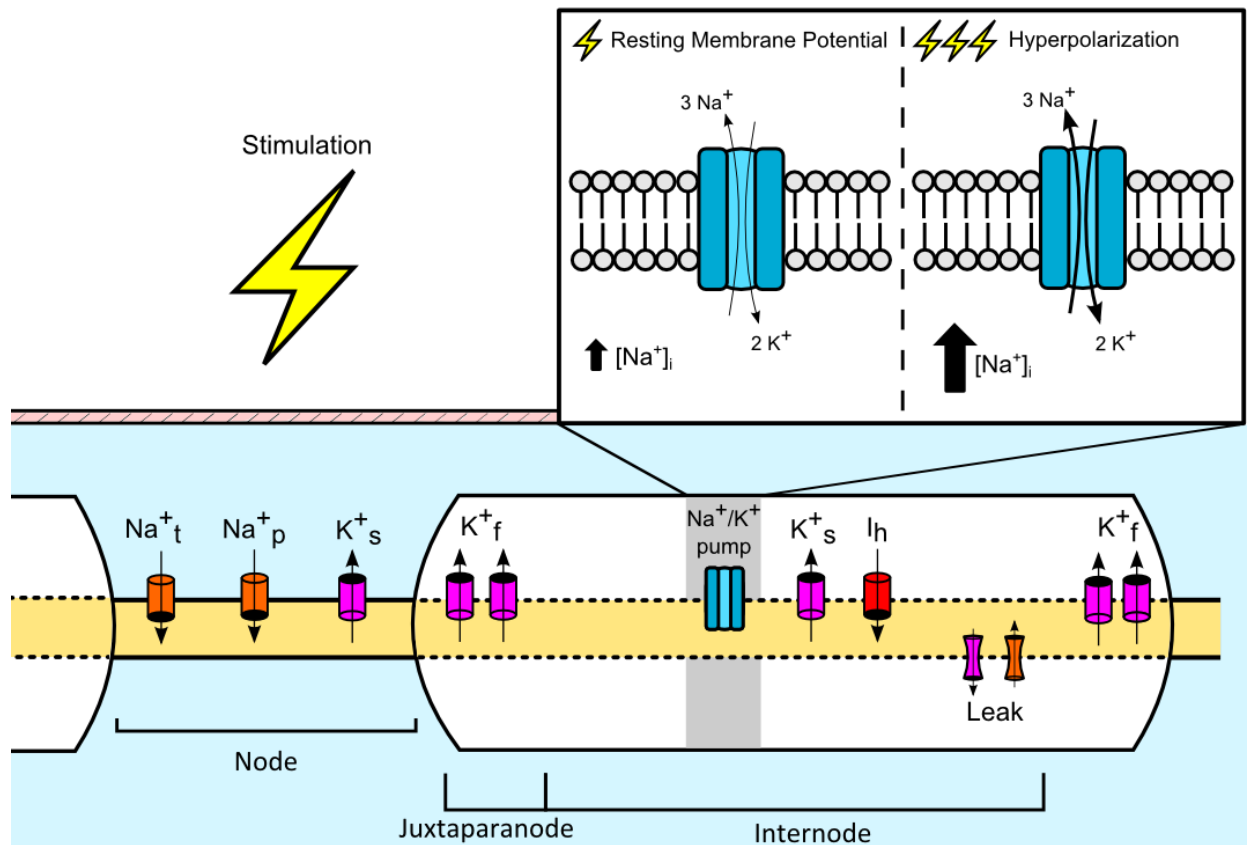


Figure 1-2. Distribution of channels across a myelinated axon. The axon is divided into the node, juxtaparanode and internode. *Inset:* Mechanism of action of membrane hyperpolarization in response to repetitive electrical stimulation

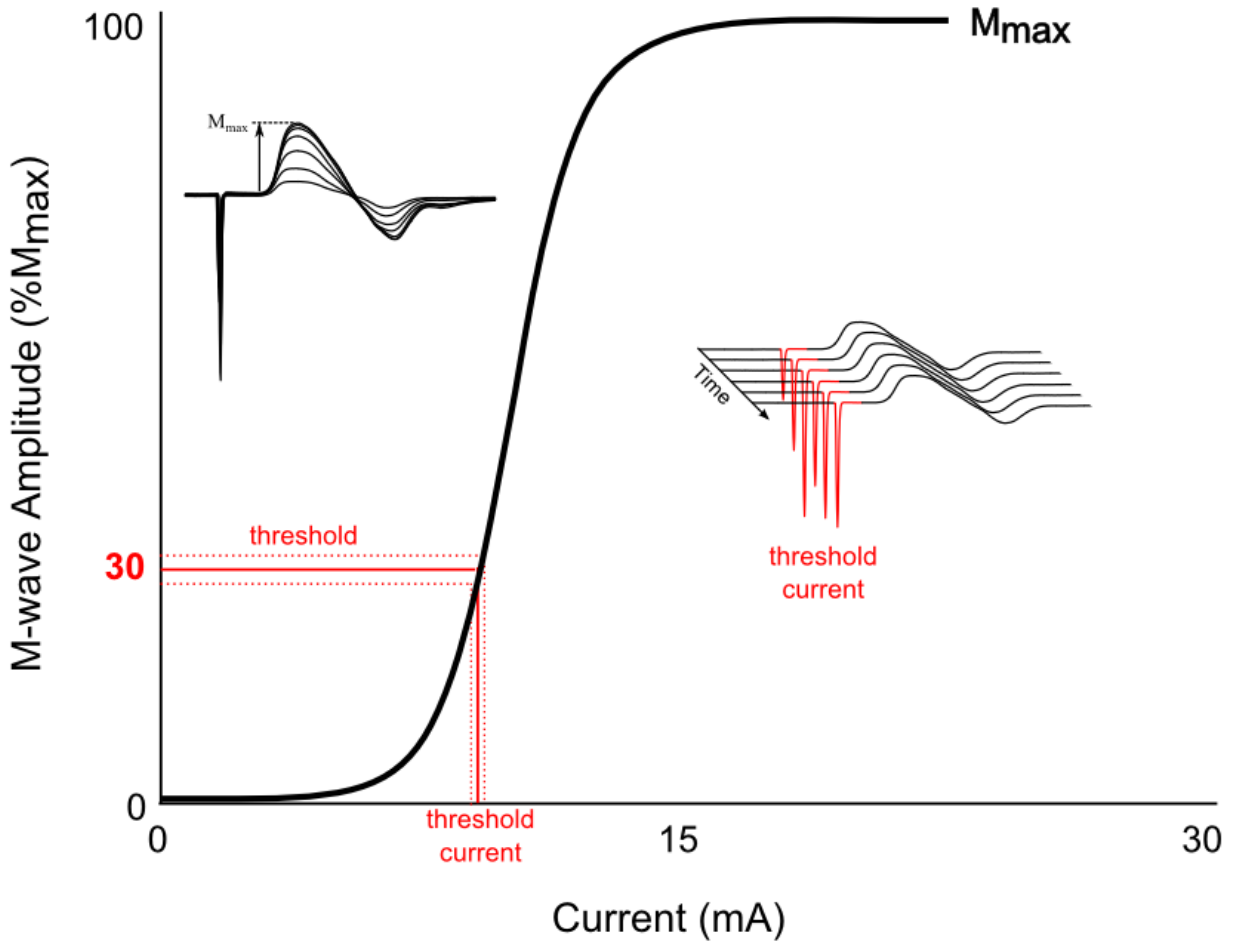


Figure 1-3. Schematic diagram of threshold tracking. A stimulus response curve (center) is generated by progressively increasing current until the measured M-wave response reaches M_{\max} as shown on the left. The tracked M-wave amplitude of 30 % M_{\max} (threshold response) and associated current (threshold current) are indicated. Right diagram shows an example of modulating the current to maintain a steady 30 % M_{\max} response.

CHAPTER 2: DECREASES IN THE EXCITABILITY OF MOTOR AXONS CONTRIBUTE SUBSTANTIALLY TO CONTRACTION FATIGABILITY DURING NEUROMUSCULAR ELECTRICAL STIMULATION

2.1. Introduction

Neuromuscular electrical stimulation (NMES) can provide many benefits when incorporated into rehabilitation programs, particularly for individuals experiencing paralysis (Maffiuletti, Roig, Karatzanos, & Nanas, 2013). Unfortunately, the use and benefits of NMES as a rehabilitation tool are limited by rapid contraction fatigability, which is characterized by a decrease in torque over time (Enoka & Duchateau, 2008). Gaining a better understanding of the mechanisms that underlie fatigability during NMES can provide a framework upon which to develop strategies to produce more fatigue-resistant contractions and improve the efficacy and outcomes of NMES-based rehabilitation programs. Currently it is generally accepted that mechanisms that contribute to contraction fatigability during NMES are limited to structures distal to and including the neuromuscular junction (NMJ).

During NMES, contractions are typically generated by the depolarization of motor axons beneath the stimulating electrodes. Accordingly, fatigability during NMES has been attributed to mechanisms distal to the stimulation site, include those that mediate neuromuscular transmission or excitation-contraction (E-C) coupling (Edwards, 1984; Jones, 1996). The breakdown of neuromuscular transmission is thought to be due to depleted neurotransmitter stores at the NMJ (Sieck & Prakash, 1995) and/or impaired depolarization of the muscle membrane (B. Bigland-Ritchie et al., 1979; Sieck & Prakash, 1995). On the other hand, the breakdown of E-C coupling is thought to be due to reduced calcium release and sensitivity (Jones et al., 1982) and accumulation

of inorganic phosphate, lactate, and reactive oxygen species (Bruton et al., 2008; Håkan Westerblad et al., 2002) within the muscle fibres (Lamb, 2009). In the present study, we test the idea that activity-dependent changes in the axons proximal to the NMJ also contribute to contraction fatigability during NMES.

It has long been known that the excitability of axons decreases when they transmit trains of action potentials (Bergmans, 1970; Bostock & Grafe, 1985). Accordingly, the ability to depolarize motor axons with an external stimulus decreases following both voluntary (Vagg et al., 1998) and electrically-evoked contractions (Kiernan et al., 2004). The implications of this decrease in excitability has gone largely underappreciated in the context of fatigability during NMES. However, when motor axons transmit a train of impulses during NMES, they become increasingly less excitable and thus motor axons “drop out” and fewer motor units (MUs) are recruited per impulse. The relationship between this decrease in axonal excitability and the drop in contraction force during NMES has not been explored previously. Changes in the excitability of motor axons can be measured from changes in current required to achieve a target M-wave amplitude (Bostock & Grafe, 1985; Burke et al., 2001; Kiernan & Lin, 2012). This, and similar “threshold-tracking” techniques, are established ways to quantify the excitability of motor and sensory axons (Kiernan et al., 2004; Kuwabara et al., 2002; Vagg et al., 1998) and examine changes in the excitability of axons in individuals with neuromuscular disorders (Krishnan et al., 2008; Lin et al., 2007; Vucic et al., 2007). Using this threshold-tracking approach, the target M-wave is referred to as the “threshold response,” while the current delivered to achieve this response is the “threshold current.” Increases in threshold current reflect decreases in axonal excitability (Bostock et al., 1998). Using this approach it is clear that changes in axonal excitability are activity-dependent;

following longer voluntary contractions (Vagg et al., 1998), and higher stimulation frequencies (Bergmans, 1970; Kiernan et al., 2004), there is both a greater decrease in axonal excitability, as well as a longer time course for recovery.

Although it has been suggested for some time that decreases in axonal excitability may contribute to contraction fatigability during NMES (Collins, 2007; Christine K Thomas, Griffin, Godfrey, Ribot-Ciscar, & Butler, 2003), only recently has experimental evidence of its contribution emerged (A. Martin et al., 2016; Matkowski et al., 2015; Papaiordanidou, Stevenot, et al., 2014). In a comparison of torque generated using supramaximal and submaximal NMES intensities, greater torque declines were found when stimulating with submaximal than supramaximal intensities (Matkowski et al., 2015; Papaiordanidou, Stevenot, et al., 2014). The difference in fatigability was attributed to reduced axonal excitability, such that the stimulus intensity during submaximal NMES was insufficient to activate the axons, consequently leading to a drop out of MUs, whereas full MU recruitment was possible with supramaximal stimulus intensities.

The primary purpose of the present study was to assess the magnitude and time course of decreases in axonal excitability during three frequencies of NMES. Changes in the excitability of motor axons were assessed by tracking the threshold current required to achieve a target M-wave amplitude of 30% the maximal M-wave (M_{max}) (Bergmans, 1970; Bostock et al., 1998; Kiernan, Burke, Andersen, & Bostock, 2000; Weigl et al., 1989). We hypothesized that the excitability of motor axons under the stimulating electrodes would decrease during NMES in an activity-dependent manner. Therefore, increases in the threshold current would be greater, occur sooner and have a longer time course for recovery as NMES frequency increased. The second purpose of

the present study was to determine the extent to which decrements in axonal excitability, neuromuscular transmission, and E-C coupling contribute to fatigability during NMES at each frequency. Thus, along with our measure of axonal excitability, supramaximal stimulation of the nerve was used to assess changes in neuromuscular transmission, while supramaximal stimuli delivered over the muscle belly were used to assess changes in E-C coupling. In the present study, contraction fatigability during NMES was modelled as a relationship between changes at the axon, NMJ, and muscle across multiple stimulation frequencies.

2.2. Methods

Experiments were conducted in the Human Neurophysiology Laboratory at the University of Alberta. All procedures were reviewed and approved by the institution's Health Research Ethics Board. Eight healthy participants (age: 30.6 ± 11.1 years; seven males) with no known neurological or musculoskeletal impairments volunteered for the present study after providing informed written consent. Participants attended three sessions, each lasting ~2 h, and separated by at least 48 h. All procedures were performed on the right leg.

Each session consisted of three phases comprised of the *Pre-fatigue*, *Fatigue*, and *Post-fatigue* phases as shown in Figure 2-1. During the *Pre-fatigue* phase, maximal voluntary contractions (MVC) of the ankle dorsiflexors and the peak twitch torque (PTT) evoked with single stimuli were assessed. Following this, a stimulus-response (S-R) curve was collected to identify M_{\max} which was then used to set the intensity of stimulation for threshold tracking measurements and measures of transmission across the NMJ that were made using a standard repetitive nerve stimulation (RNS) technique (Rich, 2006; Zivković & Shipe, 2005). Then a baseline of axonal excitability was

determined over 5 min. During the *Fatigue* phase, a fatigue protocol was delivered using one of three NMES frequencies (20, 40 or 60 Hz). The order of testing the different frequencies was randomised for each participant. The *Post-fatigue* phase followed immediately with repeated neuromuscular tests and 30 min of axonal excitability measurements. Details of the methodology are provided below.

Torque

Participants were seated in the chair of a Biodex dynamometer (System 3, Biodex Medical Systems, Shirley, New York, USA) with the right hip and knee at $\sim 120^\circ$. The right foot was securely strapped to a stationary footplate with the lateral malleolus aligned with the axis of a dynamometer and the ankle plantarflexed 10° past neutral to maximise dorsiflexion torque (Sacco, McIntyre, & Jones, 1994). The right thigh was strapped down to minimise leg movement.

Electromyography

Surface electromyography (EMG) was recorded from the tibialis anterior (TA) muscle using a pair of adhesive gel electrodes (4.8 cm^2 ; Tenby Medical, Canada) placed on the skin in a bipolar configuration (Figure 2-2). The electrodes were placed parallel to the predicted path of the muscle fibres with a $\sim 1 \text{ cm}$ inter-electrode distance. Electrodes were positioned $\sim 2/3$ of the distance between the head of the fibula and the medial malleolus. A reference electrode was placed over the tibia of the right leg. EMG signals were amplified 500-fold and band-pass filtered (0.1 – 3000 Hz; NeuroLog System; Digitimer, Welwyn Garden City, UK).

NMES

NMES was delivered through a pair of electrodes placed over the common peroneal (CP) nerve trunk (4 x 3.5 cm; Red Dot, 3M Health Care, Germany) or over the TA muscle belly (5.1 x 5.1 cm; SuperStim Premium, Richmar®, Chattanooga, TN, USA) using constant-current stimulators. Stimulation over the CP nerve was delivered using a DS5 stimulator (Digitimer, Welwyn Garden City, UK) and current was measured from its analog output. Stimulation over the TA muscle was delivered using a DS7AH stimulator (Digitimer, Welwyn Garden City, UK) and current was measured using a current probe (mA-2000, F.W. Bell). Electrodes for nerve stimulation were positioned with the cathode on the head of the fibula and the anode ~1 cm distal, along the anticipated path of the CP nerve. Electrodes for muscle stimulation were trimmed to fit over each participant's TA muscle, with the cathode positioned ~30% of the distance between the head of the fibula and the medial malleolus, and the anode ~1 cm distal (Botter et al., 2011). The electrode placements were adjusted to maximise dorsiflexion torque and minimise eversion. As stimulation of the CP nerve may activate muscles that evert or plantarflex the foot, stimulation to evoke PTT was delivered over the TA muscle. All other stimuli were delivered over the CP nerve. Skin temperature near the stimulus site was monitored and maintained between 32 – 35°C with a blanket or by applying radiant heat. All stimulus pulse durations were 0.2 ms.

Experimental Protocol

The relative timing of the various measures taken during the three phases of the experimental protocol are shown in Figure 2-1.

Pre-fatigue Phase

MVC. The *Pre-fatigue* phase started with participants performing three maximal voluntary contractions (MVCs). Each contraction lasted 2 to 3 s, with at least 1 min of rest separating contractions. Verbal encouragement and visual feedback of the torque was provided to ensure maximal activation of the muscle. The largest contraction was used as the MVC.

PTT. Following the MVCs, PTT was determined and used as a measure of the force-generating capacity of the muscle. Approximately five to ten stimuli of increasing current were delivered over the TA muscle until the minimum current that produced maximal twitch torque was found (i.e. torque no longer increased with increases in current). For subsequent PTT measurements throughout the experiment, the current was delivered at 1.3x this minimum current to ensure full activation of the muscle. In particular, we wanted to ensure that the current would be high enough to recruit any motor axons with decreased excitability. During the *Pre-fatigue* phase, three pulses of stimuli at this intensity were delivered over the TA muscle with each pulse separated by at least 5 s. The largest elicited contraction was used as the PTT.

M_{max}. The maximum M-wave (M_{max}) was determined and used as a measure of neuromuscular transmission when all motor units were activated. M_{max} was also used to set the current intensity for RNS testing and update the target M-wave to assess threshold changes during the *Fatigue* phase. The amplitude of M_{max} was determined by delivering single stimuli of increasing current over the CP nerve until a maximal response was observed. A stimulus-response curve was then constructed from responses ($n = 18 - 36$ pulses) to progressively decreasing current. The stimulus-response curve was used to establish the current required during the threshold-tracking procedure,

explained in detail below. For subsequent M_{\max} measurements and for the repetitive nerve stimulation test, the current was then set to 1.3x the minimal current required to elicit M_{\max} . As with the PTT measures, this supramaximal intensity was used to recruit all the motor axons in the CP nerve, including those with decreased excitability.

RNS. Repetitive stimulation of a nerve is a standard clinical test used to assess transmission across the NMJ (Rich, 2006; Zivković & Shipe, 2005). In our experiments, the RNS test comprised five pulses delivered over the nerve at 3 Hz and 1.3x the minimal current to elicit M_{\max} . A drop in amplitude from the first to the last M-wave of 10% or greater indicates compromised transmission across the NMJ (Ozdemir & Young, 1976). Participants rested for at least 2 min following RNS testing.

Threshold Tracking. Using the threshold tracking approach, an increase in the current required to maintain a target M-wave is indicative of a decrease in axonal excitability (Bostock et al., 1998). To establish a baseline of axonal excitability, the current required to generate an M-wave of $30 \pm 3 \%M_{\max}$ (threshold current) was measured every second for 5 min using an automated program (QTRAC, ©Institute of Neurology, London, with customised excitability protocol). This program quantifies the amplitude of each M-wave and if needed, modulates the current of the subsequent stimulus pulse to maintain the desired amplitude. All data associated with M-waves that were outside the $\pm 3\%$ margin of error were not included in data analysis or figures. This resulted in excluding 11.4% of measurements during the *Fatigue* phase.

Fatigue Phase

Contraction fatigability was induced using fatigue protocols in which NMES was delivered at 20, 40, or 60 Hz on different days. Four hundred and eighty contractions were generated over 8 min with a 0.3 duty cycle (0.3 s stimulation, 0.7 s rest). To generate the contractions for the fatigue protocols, NMES intensity was set to 1.3x the current required to produce the target M-wave of 30 % M_{\max} for the threshold tracking so that more motor axons were stimulated during the fatigue protocols than were tested using the threshold tracking technique. This ensured that axons tested during the threshold tracking were those that were recruited during the fatigue protocols. The increase of 1.3x the threshold current for the fatigue protocols was chosen based on pilot studies in which increases in the threshold current following 60 Hz NMES were less than 30%. To assess changes in neuromuscular transmission and in the force-generating capacity of the muscle throughout the fatigue protocol, single stimuli were delivered 0.3 s following every NMES train. This pulse was either a submaximal pulse over the CP nerve to measure the threshold current, or a supramaximal pulse over the TA muscle to measure PTT or over the CP nerve to measure M_{\max} . The supramaximal pulses were delivered after every fifth train in a 3:1 ratio of PTT stimuli to M_{\max} stimuli, respectively. Hence every 20 s, there were 16 threshold current measurements, three PTT measurements, and one M_{\max} measurement (see Figure 2-1, inset).

Post-fatigue Phase

Immediately after the fatigue protocol, the *Post-fatigue* phase started with a single MVC, followed by three supramaximal stimuli to measure PTT and a RNS test. These measurements were completed within 30 s. Following this, the threshold current was tracked every second for 30 min.

Data Collection and Analyses

Torque was sampled at 10 kHz using a 12-bit A/D board (National Instruments PCI 6040E, Austin, TX, USA) and custom-written Labview software (National Instruments, Austin, TX, USA). Current from the DS7AH stimulator during the *Pre-* and *Post-fatigue* phases was sampled at 20 kHz to adequately sample the current during the 0.2 ms pulse delivered over the muscle. The threshold current and M-waves were sampled at 10 kHz using a 16-bit A/D board (National Instruments USB-6251 BNC, Austin, TX, USA) and QTRAC software. Line frequency noise in the EMG was removed with a HumBug 50/60 Hz Noise Eliminator (Quest Scientific Instruments, North Vancouver, BC, Canada) before EMG data were digitised.

All data were analysed using custom-written MATLAB software (The Mathworks, Natick, MA, USA). PTT was calculated as the mean torque over a 5-ms window centred on the peak. Torque during the contractions of the fatigue protocol and MVCs were calculated as the mean over a 50-ms window centred on the peak. All M-wave amplitudes were measured baseline to peak. The amplitudes of the five M-waves during RNS were normalised to the amplitude of the M-wave generated by the first pulse (Pulse1). Threshold current data were normalised to the mean threshold current recorded during the last minute of the *Pre-fatigue* phase (see Statistics below). The threshold current data during the *Pre-* and *Post-fatigue* phases were binned over the first 15 s of each minute to generate five bins for the *Pre-fatigue* data (min -5 to -1) and 30 bins for the *Post-fatigue* data (min 9 to 38). During the *Fatigue* phase, the threshold current, M_{\max} and PTT data were binned over the first 15 s (min 0), the last 15 s (min 8) and 15 s centred on every minute (min 1 – 7).

Statistics

Statistical analyses were performed using SPSS version 23 (SPSS, Chicago, Illinois). All data were normally distributed as determined using a Shapiro-Wilk test. Comparisons of MVC, PTT and the fifth pulse of the RNS test between the *Pre-* and *Post-fatigue* phases were done using separate 2 x 3 (Time x Frequency) repeated measures analysis of variance (rmANOVA) tests. Binned threshold current was grouped into the respective phases (*Pre-fatigue*, *Fatigue*, *Post-fatigue*) and analyzed separately using two-way rmANOVAs. As no significant differences were detected across the five bins of the *Pre-fatigue* phase, the last bin (min -1) was used as the baseline measure in the ANOVA analysis to assess changes from baseline during the *Fatigue* and *Post-fatigue* phases. Separate two-way rmANOVAs were used to assess changes in binned M_{\max} , PTT and torque data during the *Fatigue* phase. Mauchly's tests were used to assess for sphericity and in cases when violated, the degrees of freedom were adjusted using Greenhouse-Geisser corrections. For all statistical tests, the significance level was set at $\alpha = 0.05$. *Post hoc* analyses with Bonferroni corrections was done for any significant main effects or interactions. To ascertain which factor (PTT or threshold current) best predicted variances in torque overall, changes in torque, PTT and current during the *Fatigue* phase were normalised to their first recorded value and a linear regression was performed across all frequencies and within individual frequencies. M_{\max} was excluded from the regression model as no evidence of impaired neuromuscular transmission occurred at any NMES frequency (see Results below). The adjusted R^2 and standardised beta coefficients with 95% confidence intervals are reported. All descriptive statistics are reported as mean \pm 1 standard deviation.

2.3. Results

Torque decreased during the 40 and 60 Hz fatigue protocols, but did not decline significantly during the 20 Hz protocol. The threshold current, that required to achieve an M-wave of 30 % M_{\max} , increased during the fatigue protocols at all three frequencies, with greater increases and longer recovery times accompanying higher NMES frequencies. There was no other evidence of decrements in neuromuscular transmission. PTT decreased only during 60 Hz NMES while the measures of PTT made before and after the fatigue protocols decreased after 40 and 60 Hz NMES.

Single Subject Data

Data recorded during the *Fatigue* phase at all three NMES frequencies in a single participant are shown in panels A-C of Figure 2-3. The top panels of Figure 2-3A show superimposed M-waves evoked by the single pulses used for threshold tracking of the M-wave at the beginning (min 0) and end (min 8) of the fatigue protocol. For this participant, M_{\max} was 7.7, 6.5 and 5.1 mV, thus the M-wave amplitudes tracked were 2.2 ± 0.2 , 1.7 ± 0.2 and 1.3 ± 0.1 mV for the 20, 40 and 60 Hz NMES sessions, respectively. The bottom panels of Figure 2-3A show superimposed torque traces from the first 15 (i.e. bin 0) and last 15 (i.e. bin 8) contractions of each fatigue protocol. Mean peak torque produced over the entire fatigue protocol is shown in Figure 2-3B. From the first to the last contraction of the fatigue protocol, torque increased 9% during 20 Hz NMES, and decreased 47% and 42% during 40 and 60 Hz NMES, respectively. As can be seen in Figure 2-3C, threshold current increased for all frequencies, rising by 13.6, 30.0 and 32.4 % of *Pre-fatigue* values during the 20, 40 and 60 Hz NMES sessions, respectively. Measurements made during the *Pre-* and *Post-fatigue* phases for this participant are shown in panels D-F of Figure 2. During the

Pre-fatigue phase, the fifth pulse of the RNS test was 100.1, 100.0 and 99.1 % of Pulse1, while during the *Post-fatigue* phase, the fifth pulse was 100.1, 99.9 and 99.4 % of Pulse1 for 20, 40 and 60 Hz NMES, respectively (Figure 2-3D). Although the stability of M_{\max} was assessed from responses to single pulses delivered during the fatigue protocols (data not shown), the M-waves from the RNS tests shown in panel D also demonstrate the stability in the amplitude of M_{\max} from before to after the fatigue protocols. There appeared to be a frequency-dependent decrease in the PTT (Figure 2-3E) and MVC (Figure 2-3F) between the *Pre-* and *Post-fatigue* data, although data for individuals was not tested for statistical significance. PTT decreased 3.9, 14.4 and 31.0% and MVC decreased 2.0, 16.7 and 20.6% following 20, 40 and 60 Hz NMES.

Group Data

Torque. The initial torque generated with 20, 40 and 60 Hz NMES was 24.3 ± 13.5 , 44.2 ± 16.3 and 56.3 ± 20.9 %MVC, respectively. There was a significant interaction between Time and Frequency ($F_{16, 112} = 13.1$, $P < 0.001$) for torque, as shown in Figure 2-4A. Torque was significantly higher during the first 2 min during 40 and 60 Hz NMES ($P = 0.001 - 0.008$) than 20 Hz NMES. There was no difference in torque produced by 40 and 60 Hz NMES throughout the protocol ($P > 0.3$). Torque dropped significantly after 4 min of 40 Hz NMES and after 3 min of 60 Hz NMES ($P = 0.03$ for both; see open symbols in Figure 2-4A). By the end of the fatigue protocol, torque decreased 48.7 ± 11.6 and 62.4 ± 16.3 % with 40 and 60 Hz NMES, respectively. Torque did not change over the course of the 20 Hz fatigue protocol as there were no differences between min 0 and any of the subsequent bins (min 1 – 8; $P = 1.0$).

M_{max}. There was no interaction ($F_{16, 112} = 0.8, P = 0.7$) or main effect of Frequency ($F_{2,14} = 0.4, P = 0.7$; Figure 2-4B) for M_{\max} but there was a main effect of Time ($F_{8, 56} = 8.3, P < 0.001$).

Independent of NMES frequency, M_{\max} was significantly higher during min 7 compared to the beginning of the *Fatigue* phase, increasing from 6.2 ± 2.0 to 6.6 ± 2.2 mV ($P = 0.04$).

PTT. There was a significant interaction between Time and Frequency for PTT ($F_{16, 112} = 10.6, P < 0.001$; Figure 2-4C). PTT at the beginning of the *Fatigue* phase (min 0) was $11.3 \pm 3.9, 13.5 \pm 4.4$ and 15.5 ± 5.9 %MVC for 20, 40, and 60 Hz NMES, respectively. There were no significant differences in PTT at min 0 between NMES frequencies ($P = 0.1 - 0.7$). However, PTT was significantly lower after 4 min of 40 and 60 Hz NMES ($P = 0.01 - 0.05$) than 20 Hz NMES. By the end of the *Fatigue* phase, PTT was $12.3 \pm 6.7, 7.9 \pm 3.0$ and 6.7 ± 5.4 %MVC for 20, 40 and 60 Hz NMES, respectively. PTT decreased significantly after 2 min of 60 Hz NMES ($P = 0.03$). PTT did not change significantly during the 20 or 40 Hz fatigue protocols ($P > 0.1$ for all time-wise comparisons).

Threshold Current. Figure 2-5 shows the change in current required to produce an M-wave of 30 % M_{\max} over time across the group of eight participants. Separate rmANOVAs were run on data from the three phases of the experiment. The mean current used for threshold tracking during the *Pre-fatigue* phase was 13.5 ± 8.0 mA. Threshold current did not change significantly during the *Pre-fatigue* phase; there were no interactions ($F_{10, 70} = 0.4, P = 0.9$) or main effects of Frequency ($F_{2,14} = 0.2, P = 0.8$) or Time ($F_{1.7, 12.1} = 0.4, P = 0.9$) for the threshold current during that phase. During the *Fatigue* phase, the mean current used to produce the NMES trains was $18.7 \pm 12.1, 17.7 \pm 10.8$ and 17.1 ± 10.2 mA for 20, 40 and 60 Hz NMES, respectively. This

current evoked M-waves of 79.9 ± 7.5 , 61.3 ± 14.1 and 71.3 ± 12.2 % M_{\max} at the beginning of the 20, 40 and 60 Hz NMES fatigue protocols, respectively. There was a significant Time by Frequency interaction ($F_{2,3,16,2} = 12.4$, $P < 0.001$) for the threshold current during the *Fatigue* phase. The threshold current significantly increased after 1 min during both 20 and 40 Hz NMES ($P = 0.008$ and 0.009 , respectively) and after 2 min of 60 Hz NMES ($P = 0.03$; see open symbols in Figure 2-5). By the end of the fatigue protocol, the threshold current increased 13.5 ± 3.2 ($P < 0.001$), 27.4 ± 4.5 ($P < 0.001$) and 34.6 ± 5.8 % ($P < 0.001$) after 20, 40 and 60 Hz NMES, respectively. This threshold current was 2.6 ± 2.2 , 0.2 ± 0.5 and 0.2 ± 0.9 mA below the current used to produce the NMES trains for 20, 40 and 60 Hz NMES, respectively.

Between frequencies, the threshold current was significantly higher than 20 Hz after 2 min of 60 Hz ($P = 0.008$) and after 3 min of 40 Hz NMES ($P = 0.001$), while 60 Hz was higher than 40 Hz after 6 min ($P = 0.02$). During the *Post-fatigue* phase, there was a significant interaction between Time and Frequency ($F_{60, 420} = 7.4$, $P < 0.001$). The threshold current measured during the *Post-fatigue* phase was not significantly different than the *Pre-fatigue* phase immediately following 20 Hz, 2 min after 40 Hz and 4 min after 60 Hz NMES.

Pre- versus Post-fatigue Measures

Figure 2-6 shows mean group data for measures made during the *Pre-* and *Post-fatigue* phases. Figure 2-6A shows torque generated by the MVCs during the *Pre-* (open circles) and *Post-fatigue* (closed circles) phases. There was a significant interaction between Frequency and Time for MVC torque ($F_{2, 14} = 6.9$, $P = 0.008$). There were no differences in torque produced by the MVCs generated during the *Pre-fatigue* phase between frequencies ($F_{2, 14} = 0.6$, $P = 0.6$). For all

frequencies, MVCs produced significantly less torque after the fatigue protocol (*Post-fatigue*) than before it (*Pre-fatigue*) ($F_{1,7} = 33.6, P = 0.001$). During the *Post-fatigue* phase, less torque was generated during MVCs after the 60 Hz fatigue protocol than those after the 20 Hz protocol.

Changes in PTT between the *Pre-* and *Post-fatigue* phases are shown in Figure 2-6B. There was a significant Frequency by Time interaction for PTTs generated during the *Pre-* and *Post-fatigue* phases ($F_{2,14} = 7.8, P = 0.005$). There was no difference in PTT during the *Pre-fatigue* phase ($F_{2,14} = 0.009, P = 1.0$ between all three frequencies) eliciting 3.3 ± 1.0 Nm (9.0 ± 2.6 %MVC). During the *Post-fatigue* phase, PTT decreased significantly to 2.4 ± 1.0 ($P = 0.03$) and 1.7 ± 1.1 Nm ($P = 0.001$) following 40 and 60 Hz NMES, respectively. During the *Post-fatigue* phase, PTT was smaller after the 60 Hz fatigue protocol than the 20 Hz protocol.

Across all frequencies, the fifth pulse of the RNS test was 99.9 ± 0.6 and 99.8 ± 0.6 % of Pulse1 during the *Pre-fatigue* and *Post-fatigue* phases, respectively (Figure 2-6C). There was no significant interaction ($F_{2,14} = 1.4, P = 0.3$) or main effect of Frequency ($F_{2,14} = 1.5, P = 0.3$) or Time ($F_{1,7} = 0.3, P = 0.6$) for the relative change in M-wave. These values were also well below the 10% decrement as noted in the literature (Ozdemir & Young, 1976) signifying impaired NMJ function.

Regression Analyses

A standard multiple regression analysis was done to determine if torque could be predicted by two independent variables: PTT and threshold current. Across the three NMES frequencies the overall fit of the model was moderate to strong, 62.4% of the variance was explained, with PTT

and threshold significantly predicting torque ($F_{2, 213} = 176.5, P < 0.001$; Table 1). The relative contribution of the predictor variables was determined by the absolute value of the beta-coefficients and the overlap of its 95% confidence intervals. Changes in torque during the fatiguing NMES protocol were more sensitive to changes in threshold current ($\beta = -0.57 [-0.65, -0.47]$) compared to PTT ($\beta = 0.36 [0.27, 0.45]$), indicating a stronger relative contribution of threshold current. There was no significant decrease in torque when NMES was delivered at 20 Hz and the model explained only 16.7 % of the variance in torque during the 20 Hz fatigue protocol ($F_{2,69} = 8.4, P = 0.001$) (Figure 2-7A). For data from the 40 and 60 Hz NMES sessions, the model explained 72.0 ($F_{2,69} = 91.7, P < 0.001$) (Figure 2-7B) and 74.0 % ($F_{2,69} = 80.3, P < 0.001$) (Figure 2-7C) of the variance in torque, respectively. At each frequency, there was no significant difference in the predictive weights of changes in threshold current and PTT on decreases in torque (Figure 2-8). With 40 Hz NMES, changes in threshold current had a beta coefficient of -0.58 [-0.72, -0.43] and PTT had a beta coefficient of 0.41 [0.27, 0.55]. With 60 Hz NMES, the relative predictive weights of threshold current and PTT were $\beta = -0.51 [-0.65, -0.37]$ and $\beta = 0.58 [0.44, 0.72]$, respectively.

2.4. Discussion

We have shown that decreases in the excitability of motor axons under the stimulating electrodes contribute substantially to contraction fatigability during NMES. Consistent with our hypothesis, the decrease in excitability was frequency-dependent; higher NMES frequencies produced greater decreases in axonal excitability as evidenced by greater increases in threshold current. Overall across the three frequencies (20, 40, 60 Hz), decreases in axonal excitability were a stronger predictor of the decline in torque during the fatigue protocols. No significant changes

were observed during RNS testing or in M_{\max} for any of the frequencies tested, providing strong evidence that neuromuscular transmission was not compromised under the current experimental conditions.

In the present study, torque declined during 40 and 60 Hz NMES but not during 20 Hz NMES, consistent with previous evidence that contraction fatigability during NMES depends on stimulation frequency (Behringer et al., 2016; Papaiordanidou, Billot, Varray, & Martin, 2014; Sacco et al., 1994). The lack of contraction fatigability during 20 Hz NMES was not unexpected as the low stimulation frequency falls within the physiological discharge range of TA motor units (Connelly et al., 1999). Interestingly, although threshold current increased by approximately 14% during 20 Hz NMES, this did not lead to a decrease in torque. Thus, force produced by the muscle was preserved despite a drop-out of motor units associated with decreased axonal excitability. For example, low frequency NMES can potentiate force output by a hypothesized increase in myofibrillar calcium sensitivity (Gibson, Cooper, Stokes, & Edwards, 1988). However, our measure of PTT was not sensitive to detect force potentiation during 20 Hz NMES (Figure 2-4C).

Indirect evidence that decreases in axonal excitability may contribute to decreases in torque during NMES was recently provided by comparisons of the mechanical and electrophysiological properties of twitches elicited during a fatigue protocol (A. Martin et al., 2016; Matkowski et al., 2015; Papaiordanidou, Stevenot, et al., 2014). In the present study, a threshold tracking technique was used to directly measure changes in the excitability of motor axons under the stimulating electrodes. An underlying assumption inherent to this approach is that a change in

the M-wave is due to a change in motor axons (Bostock et al., 1998; Weigl et al., 1989). However, several factors can influence M-wave amplitude other than the number of axons recruited by a peripheral nerve stimulus. Impaired transmission across the NMJ (Desaulniers, Lavoie, & Gardiner, 2002; Rich, 2006), and ionic changes in the muscle affecting action potential propagation along the sarcolemma, influence the size of the M-wave (Badier, Guillot, Danger, Tagliarini, & Jammes, 1999; Hicks & McComas, 1989). We found no change in either the RNS tests or the amplitude of M_{max} at any frequency, providing evidence that neuromuscular transmission was intact and there were no decrements in transmission across the NMJ or in the genesis and propagation of action potentials along the muscle membrane. Taken together, the increases in threshold current along with no other evidence of decrements in neuromuscular transmission provide strong evidence that the changes in threshold current reflect decreases in the excitability of the motor axons (Bostock et al., 1998). Such an activity-dependent decrease in excitability may be due to a decrease in sodium currents as a result of channel inactivation (Choi et al., 2006) or hyperpolarization of the axonal membrane due to over activity of the electrogenic sodium-potassium pump (Bergmans, 1970; Bostock et al., 1998; Kiernan et al., 2004; Vagg et al., 1998; Weigl et al., 1989).

Our result of a greater increase in threshold current with higher stimulation frequencies is consistent with data from single human motor axons (Bergmans, 1970) and previous literature on the activity-dependence of decreases in the excitability of axons in the median nerve (Kiernan et al., 2004; Vagg et al., 1998). Compared with the median nerve, the CP nerve has less pronounced increases in the threshold current following sustained MVCs, attributed to differences in the complement of ion channels and sodium-potassium pump activity between the two nerves

(Kuwabara et al., 2000, 2002). Accordingly, the magnitude and time course of increases in the threshold current appear to be nerve-dependent. In the latter half of the fatigue protocol, the rate of increase in the threshold current became progressively smaller, a result observed across all frequencies. This finding is supported by Kiernan *et al* (Kiernan et al., 2004), who suggested a ceiling effect when cutaneous afferents stimulated at 20 and 30 Hz showed similar decreases in excitability levels. This may be caused by saturation of the sodium-potassium pump activity (Clausen, 1996) which is largely responsible for axonal hyperpolarization following prolonged stimuli trains, leading to decreases in axonal excitability (Bergmans, 1970; Bostock & Grafe, 1985).

The second objective of the present study was to assess the relative contribution of: axon excitability, neuromuscular transmission and the force-generating capacity of the muscle, to predicting changes in torque output during the NMES fatigue protocols. Previous literature has suggested that fatigability during NMES was caused by impaired neuromuscular transmission or a breakdown in E-C coupling (Jones, 1996). Mechanisms impairing neuromuscular transmission include depletion of readily-releasable transmitter stores at the NMJ (Sieck & Prakash, 1995) and depletion of sodium and buildup of potassium extracellular to the muscle membrane (Jones et al., 1979). Whereas E-C coupling can breakdown due to reduced calcium release and re-uptake from the sarcoplasmic reticulum, and damage to the sarcomeres (Jones, 1996; Keeton & Binder-Macleod, 2006). In the present study, decrements in PTT were attributed to impairments in the force-generating capacity of the muscle. This conclusion is contingent on the uncompromised transmission across the NMJ, as evidenced by the RNS test, and action potential propagation along the muscle fibres, as evidenced by an absence of change in M_{max} . Altogether, we attribute

the torque declines during NMES both to decreased axonal excitability and impaired force-generating capacity of the muscle. The regression model revealed that up to 75% of the torque decrease was accounted for by increases in the threshold current and decreases in the muscle's contractile capacity during NMES at both 40 and 60 Hz. The relative weights of each predictor variable were independent of frequency, having similar contributions to decreases in torque during 40 and 60 Hz NMES.

In the present study, we opted to match stimulus intensity across the NMES protocols to ensure that a similar number of axons were recruited per impulse, rather than contraction amplitude which would result in fewer axons recruited at higher NMES frequencies. This led to NMES delivered at 40 and 60 Hz generating approximately two-fold greater torque as NMES at 20 Hz. The goal of the present study was to compare the activity-dependence of threshold changes, thus differences in its time course across protocols would only be dependent on the number of action potentials propagating within each axon.

The present results demonstrate that decreases in the excitability of motor axons beneath the stimulating electrodes is a significant contributor to fatigability overall. "Fatigability" that develops because axons drop-out as they become less-excitabile is counter-productive for NMES based-programs, whether the goal is to promote muscle strengthening or to restore movement. Strategies designed to minimize decreases in axonal excitability may optimise the benefits of such NMES-based programs. One such strategy to minimise decreases in axonal excitability during NMES involves distributed NMES techniques which rotate stimulus pulses between multiple stimulating electrodes over the muscle belly (Popović & Malešević, 2009), or over a

muscle belly and nerve trunk (Lou, Bergquist, Aldayel, Czitron, & Collins, 2017), to recruit unique motor unit populations from each stimulation site and reduce motor unit firing rates thus producing more fatigue-resistant contractions (Barss et al., n.d.). Reducing the extent of axonal excitability decreases will effectively increase the activation of the muscle throughout and increase the efficacy of NMES-based programs.

2.5. Figures

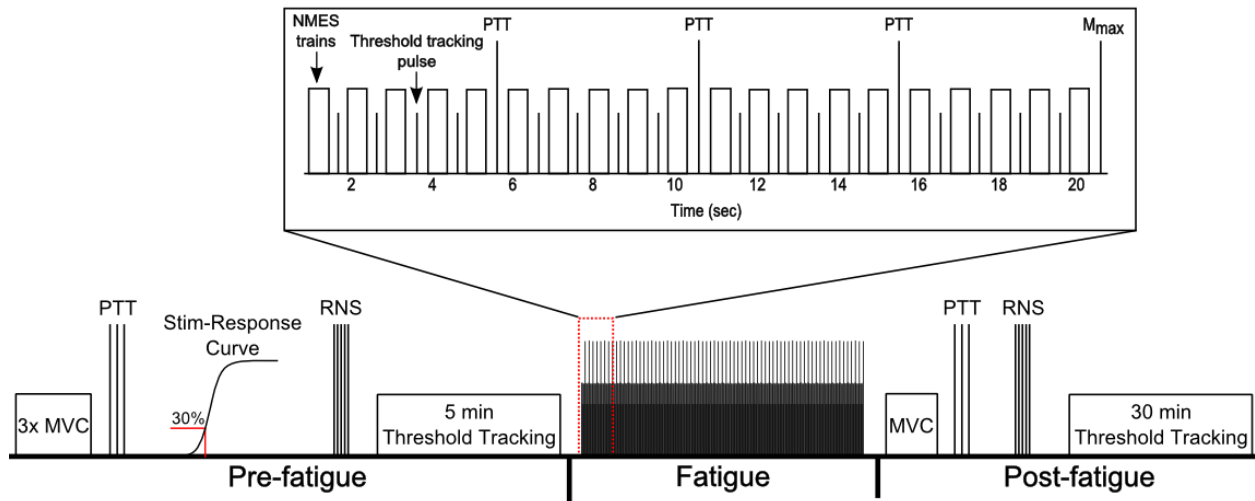


Figure 2-1. Schematic description of the experimental protocol. Each session was comprised of three phases: *Pre-fatigue*, *Fatigue*, and *Post-fatigue*. The inset shows an expanded view of the first 20 s of the fatigue protocol, indicating the timing of threshold tracking and supramaximal pulses following each NMES train.

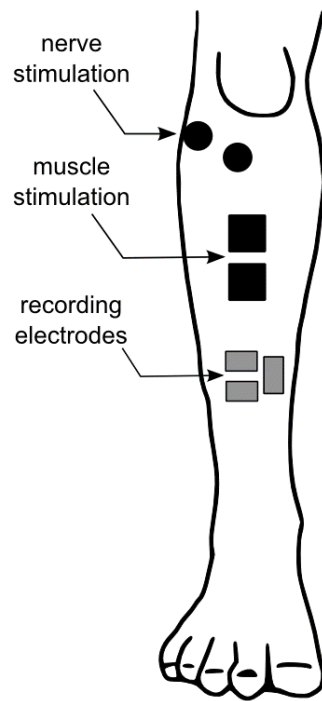


Figure 2-2. Electrode placement for nerve and muscle stimulation.

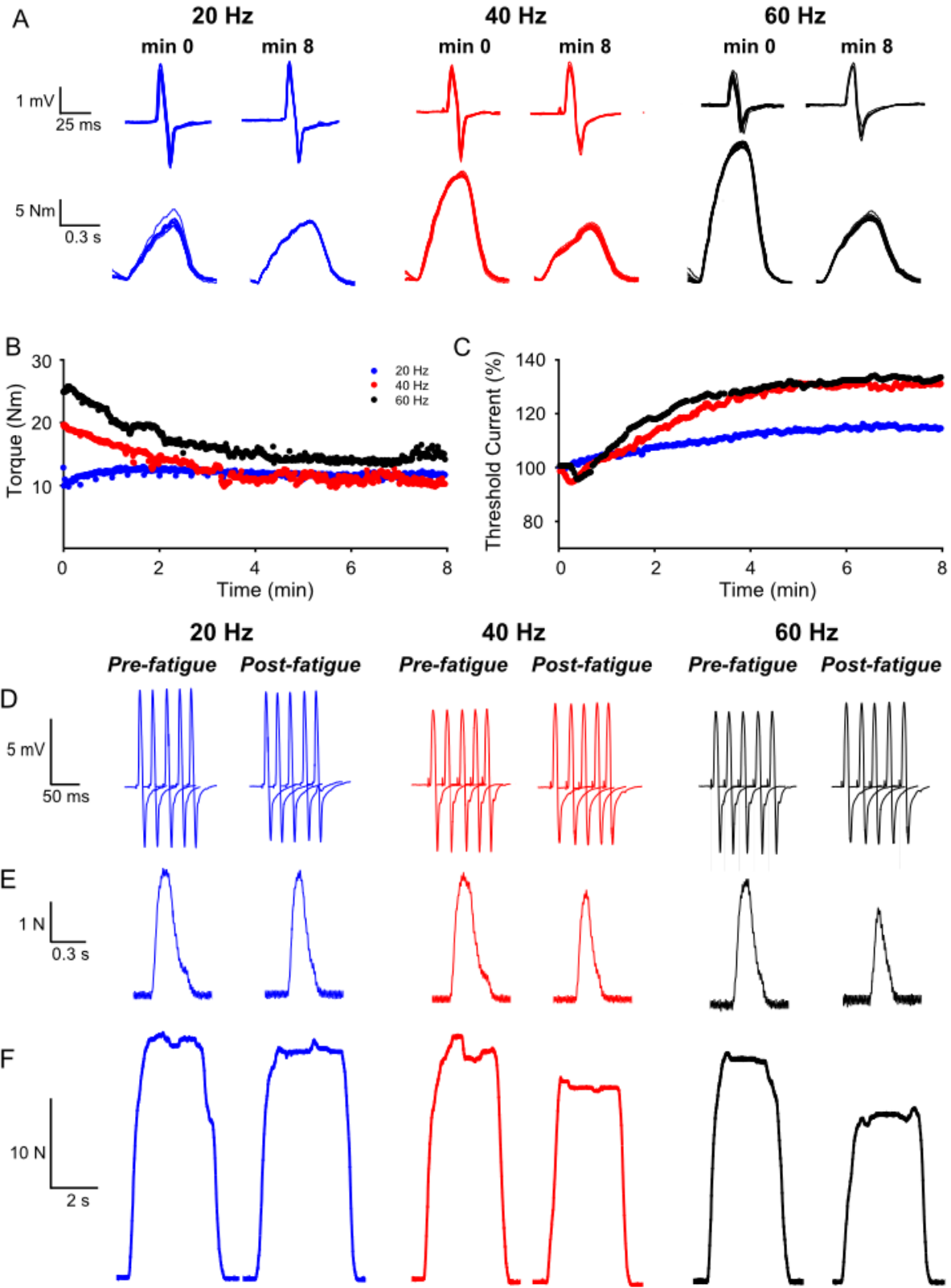


Figure 2-3. Representative data from a single participant at each of the three NMES frequencies. A) The tracked M-waves (top) and torque generated by the NMES trains (bottom) during the *Fatigue* phase. Data show the superimposed traces ($n = 15$) from the first (left) and last (right) bin of the phase. The time course of changes in B) torque and C) threshold current elicited from NMES trains delivered at 20, 40 and 60 Hz during the *Fatigue* phase. Every 5th point is shown in (B) and (C) for clarity. Data from the *Pre-* and *Post-fatigue* phase showing D) overlaid M-waves during repetitive nerve stimulation, E) peak twitch torque and F) maximal voluntary contractions.

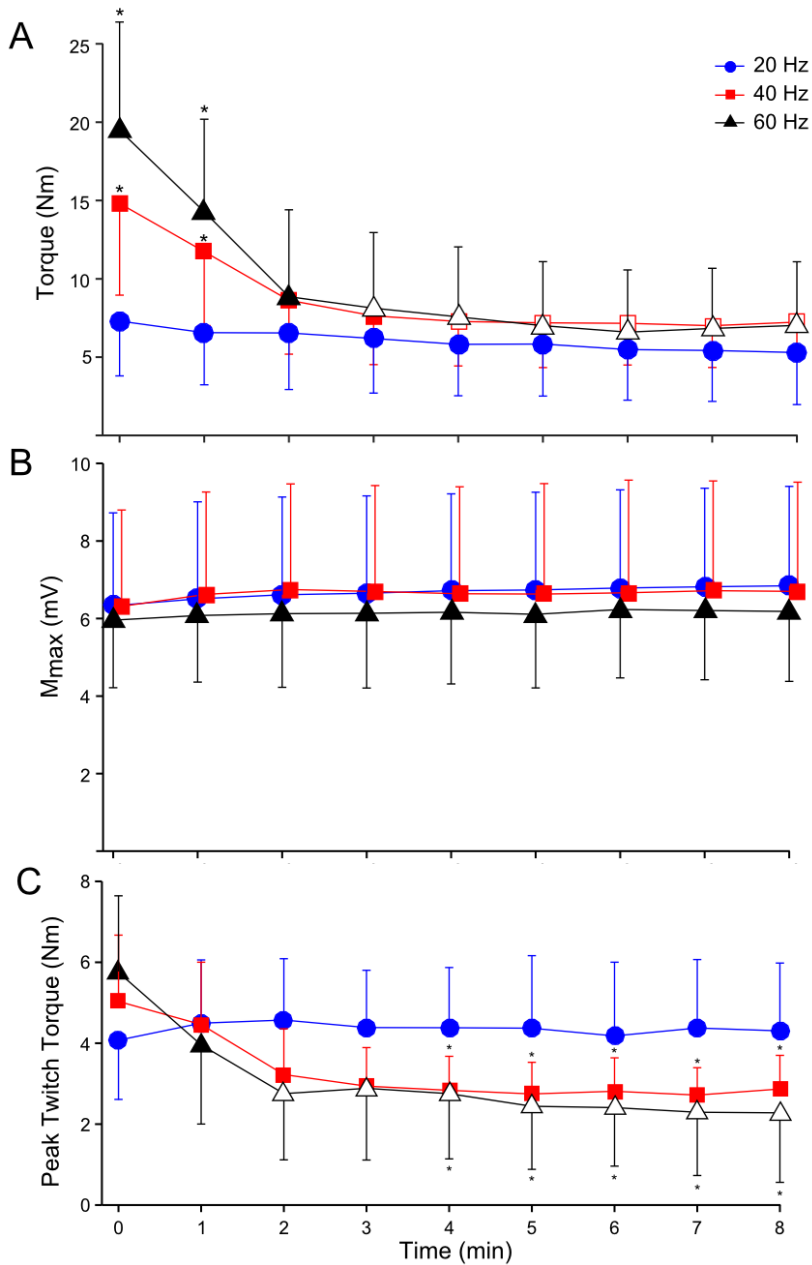


Figure 2-4. Binned A) train torque output, B) M_{\max} amplitude, and C) PTT during the fatigue protocol for each frequency. All data are expressed as mean \pm SD ($n = 8$). The open symbols indicate significant differences from the first bin across Time ($P < 0.05$). Asterisk (*) denotes when both 40 and 60 Hz groups are significantly different relative to 20 Hz ($P < 0.05$).

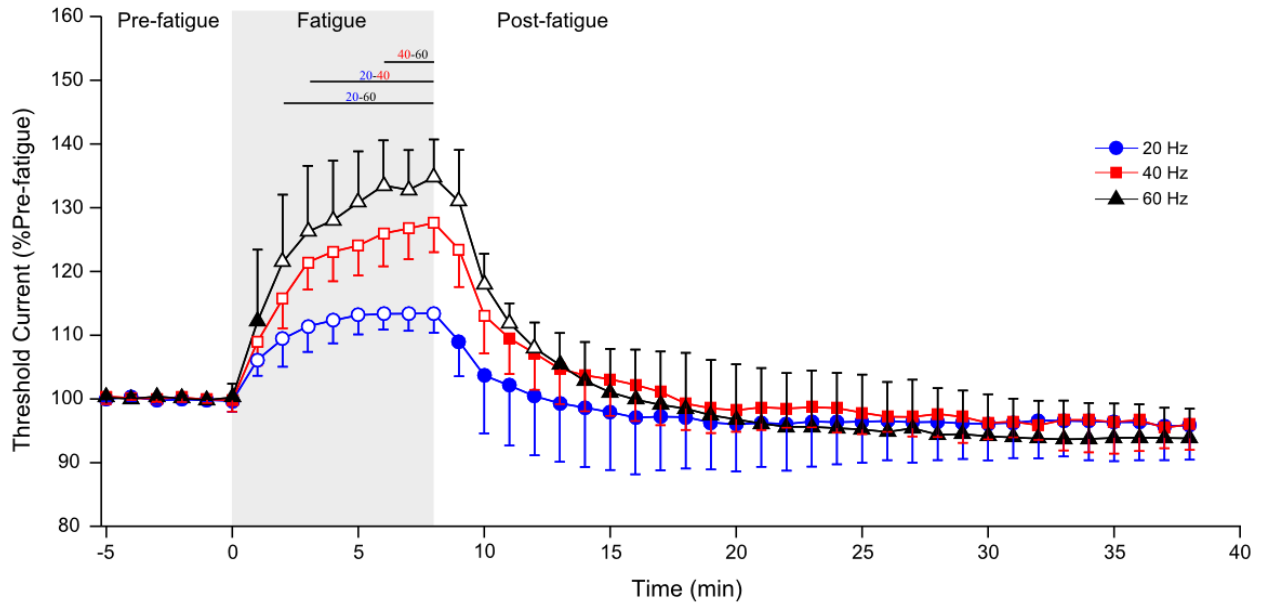


Figure 2-5. Binned threshold current normalized to the mean across the *Pre-fatigue* phase. All data are expressed as mean \pm SD ($n = 8$). The shaded area denotes the *Fatigue* phase. The open symbols denote significant increases from values recorded during the *Pre-fatigue* phase across Time ($P < 0.05$). Asterisks (*) denote significant timewise comparisons between frequencies as indicated by the pair of symbols ($P < 0.05$).

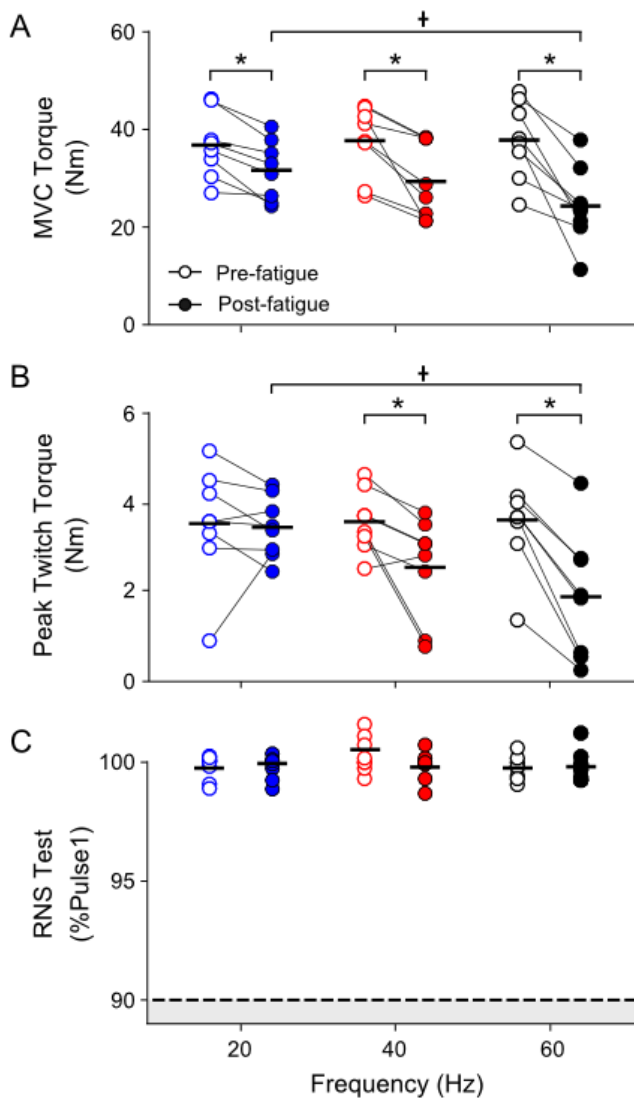


Figure 2-6. Mean (bold horizontal lines; $n = 8$) and individual participant (circles) data showing A) MVC and B) potentiated PTT before (empty circles) and after (filled circles) the fatigue protocol at each NMES frequency. The last pulse of the RNS test before (empty) and after (filled) the fatigue protocol are shown in (C). The dotted line represents a 10% decrement denoting a compromised NMJ. The 5th pulse of the RNS test is normalized to the 1st pulse. Asterisks (*) denote a significant decrease across Time ($P < 0.05$). Dagger (†) denotes a significant difference across Frequency ($P < 0.05$).

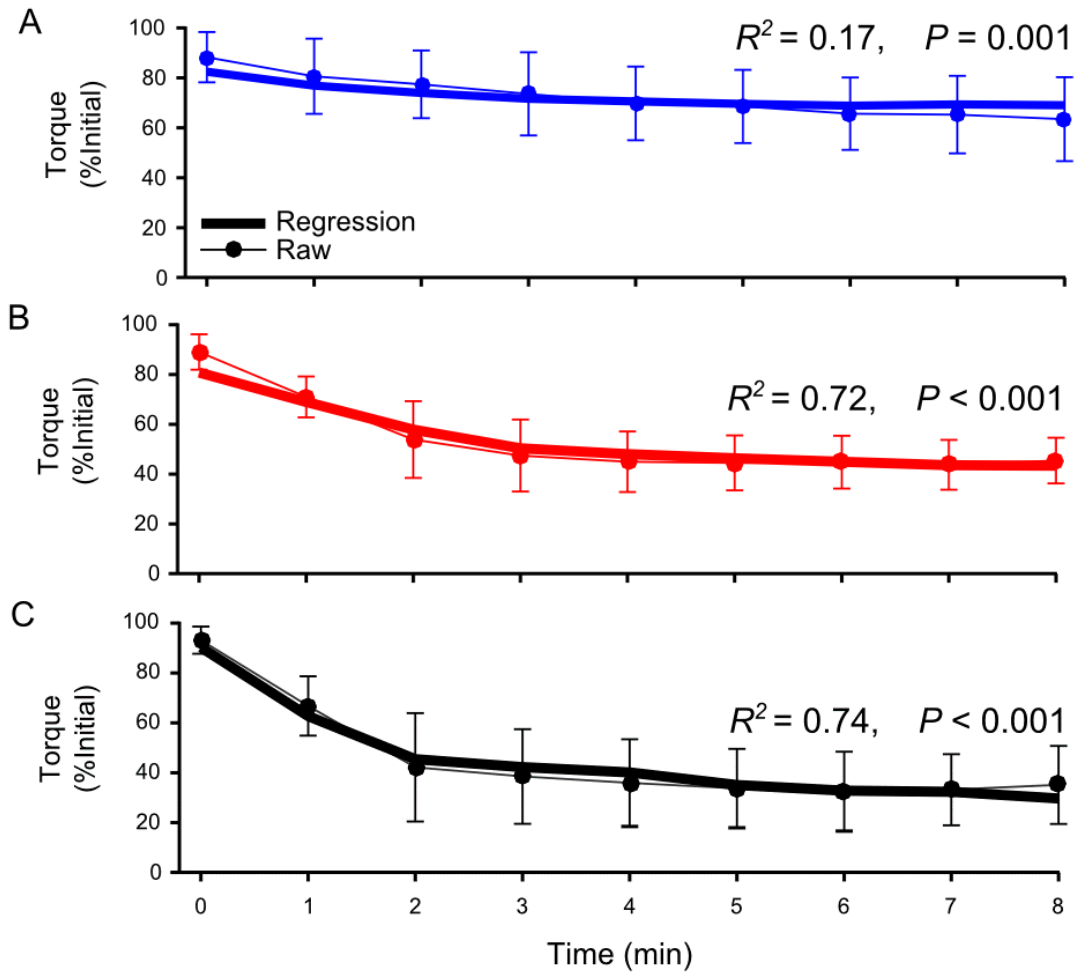


Figure 2-7. Linear regression relationship for torque evoked with A) 20 Hz ($R^2 = 0.17$, $P = 0.001$), B) 40 Hz ($R^2 = 0.72$, $P < 0.001$) and C) 60 Hz ($R^2 = 0.74$, $P < 0.001$), related to PTT and threshold current. Thick lines show the predicted torque based on the regression model. Solid circles with thin lines show the binned torque data. All data expressed as mean \pm SD ($n = 8$).

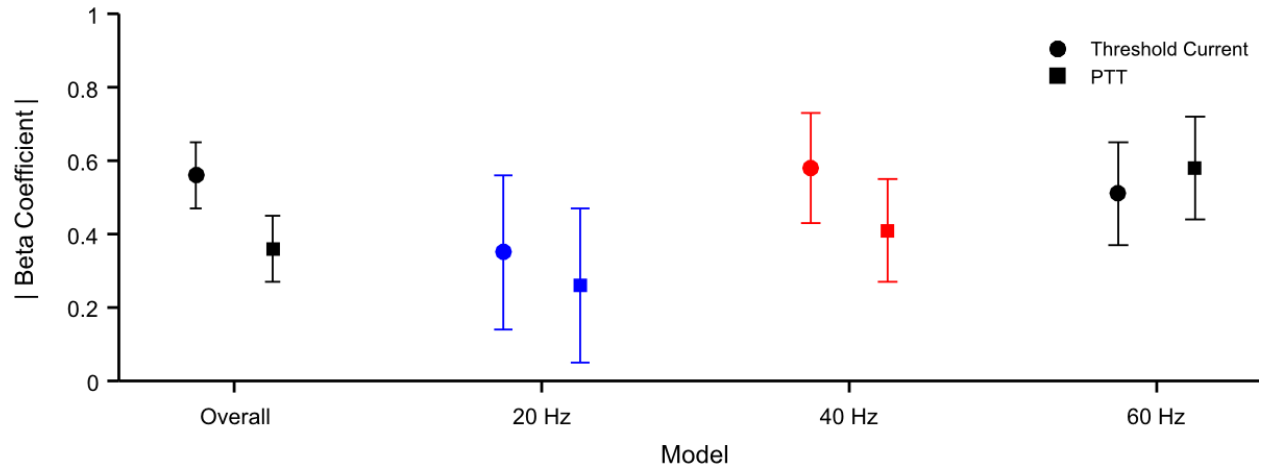


Figure 2-8. Beta coefficients for the relative predictive weights of threshold current (circle) and PTT (square) for each linear regression model. All data are expressed as $\beta \pm 95\%$ confidence intervals.

2.6. Tables

Table 2-1. Multiple linear regression model for the effect of increases in threshold current and decreases in PTT on decreases in torque.

Model	Adjusted R ²	Variable	β	95% CI		P-value
Overall	0.62	Current	0.56	0.47	0.65	<0.001
		PTT	0.36	0.27	0.45	<0.001
20 Hz	0.17	Current	0.35	0.14	0.57	0.002
		PTT	0.26	0.04	0.47	0.02
40 Hz	0.72	Current	0.58	0.43	0.72	<0.001
		PTT	0.41	0.27	0.55	<0.001
60 Hz	0.74	Current	0.51	0.37	0.65	<0.001
		PTT	0.58	0.44	0.72	<0.001

CHAPTER 3: GENERAL DISCUSSION

The primary purpose of the present study was to investigate the magnitude and time course of changes in axonal excitability during neuromuscular electrical stimulation (NMES) delivered at three frequencies to the tibialis anterior (TA) muscle in neurologically intact individuals. Secondly, the extent to which changes in the axon, neuromuscular junction (NMJ) and muscle contribute to contraction fatigability during NMES at each frequency was examined. In this chapter, I first expand on the mechanisms that contributed to contraction fatigability under the current conditions of the present study. I then discuss the various safety factors that are involved in generating a contraction. Finally, the clinical implications and limitations of the current work are presented, concluding with potential future directions for the present work.

3.1. Contraction Fatigability

As mechanisms contributing to contraction fatigability can be described as “task dependent,” we narrowed the scope of the present study to fatigability resulting from intermittent submaximal electrical stimulation, similar to that used during rehabilitation (Berkelmans, 2008). Previously, fatigability during electrically-evoked contractions has been dissociated into neuromuscular transmission failure (NTF) or a breakdown in the excitation-contraction coupling mechanism (Edwards, 1984; Jones, 1996). In the present study, we found that neuromuscular transmission failure did not play a role in fatigability. During the fatigue protocol, we regularly measured the maximal M-wave (M_{max}) as a measure of neuromuscular transmission and updated the threshold-tracking target accordingly to excite 30% of the current maximal signal. Decreases in neuromuscular transmission have previously been argued as a prominent component to

fatigability, particularly during electrically-evoked contractions (Aldrich et al., 1986; B. Bigland-Ritchie et al., 1979; Pagala, Namba, & Grob, 1984), thus we expected to observe some decrements in M_{\max} ; however, other studies have noted that even if the muscle action potential declines, the associated force decrease was not proportional when investigated in animal experiments (Balog, Thompson, & Fitts, 1994; Lüttgau, 1965). Experimental conditions such as the bathing solution (Hicks & McComas, 1989) and electrode recording set-up (Pagala et al., 1984) have been suggested to contribute to the unclear understanding of the contribution of NTF to fatigability. In the present study, we conclude that NTF is not a contributor to fatigability during NMES in humans.

Under the conditions of our study, it was a combination of both decreases in axonal excitability and a breakdown in excitation-contraction coupling which were the strongest predictors of fatigability. Both increases in threshold current and decreases in tetanic torque followed a similar time course at both 40 and 60 Hz, with rapid changes occurring over the first few minutes followed by more gradual changes. Physiologically, the pattern of change may be well related. It was found that axons innervating fast MUs in rats may be more susceptible to hyperpolarization because of reduced I_H currents – a depolarizing current that activates in response to hyperpolarization (Lorenz & Jones, 2014). In the TA, approximately 70% of the muscle fibres are type I fibres (Johnson, Polgar, Weightman, & Appleton, 1973). Following repetitive stimulation, the axons that are more prone to “dropping out” may be those that innervate fast-fatigable MUs and thus there is an initial rapid reduction in torque and increase in threshold current; while those axons innervating the fatigue-resistant MUs comprise the gradual decrease in torque and increase in current.

3.2. Safety Factors of Generating Contractions

Several safety mechanisms have been identified that ensure reliable activation and contraction of the muscle during even the most extreme human movements, further lending evidence that the rapid changes observed in the present study are due to changes in the number of recruited axons. Using an *ex vivo* preparation of a frog motor nerve, Tasaki (1953) found that the current generated at one node of Ranvier can be reduced up to 1/7 of its original magnitude before conduction is blocked at successive nodes. Thus, the author concluded that under physiological conditions, the current developed at each node of Ranvier is 5 – 7 times stronger than required to depolarize successive nodes along the axon (Tasaki, 1953), though this value may be reduced at regions of axonal bifurcation (Krnjevic & Miledi, 1959). The safety factor at the NMJ can be defined as the ratio between the released number of quanta containing acetylcholine to the number required to depolarize the muscle membrane and has been estimated to be between 2 – 5 in adult mammals (Wood & Slater, 2001). However, the size of the readily releasable quanta pool, number of quanta released per impulse, and activation threshold at the muscle membrane is dependent on the muscle and activation patterns of that muscle (Ermilov, Mantilla, Rowley, & Sieck, 2007; Reid, Slater, & Bewick, 1999). Within the excitation-contraction elements of the muscle, studies have shown that at high stimulation frequencies, the action potential observed in the muscle may decrease sooner than the mechanical response (Cooper, Edwards, Gibson, & Stokes, 1988; Lüttgau, 1965). Cooper et al. (1988) observed greater reductions in M_{\max} amplitude relative to tetanic torque during supramaximal stimulation of the ulnar nerve at frequencies higher than 50 Hz. The authors attributed the preserved force output from the muscle to elevated calcium concentrations in the myoplasm despite excitation failure.

3.3. Clinical Implications

Currently, it is common practice to progressively increase the current to maintain the desired output as fatigability develops. The results of this experiment suggest that progressively increasing the current approximately 30% effectively combats changes in threshold current during NMES at 40 Hz, re-recruiting MUs that have “dropped out” due to increases in their activation threshold. Another finding of this experiment is that the increase in threshold current is dependent on NMES frequency. Therefore, reducing the discharge rates of individual MUs by distributing NMES among multiple stimulating electrodes would decrease the extent to which decreases in axonal excitability occurs thus reducing fatigability.

3.4. Limitations

In addition to the limitations discussed in Chapter 2, another includes a lack of detailed analysis regarding the different ion channels along the membrane, which typically accompanies threshold-tracking measurements. As the primary interest of the present study was in the time course of changes occurring in the muscle and nerve during fatigability, the lack of time between successive NMES trains did not allow for tracking other excitability parameters, such as the strength-duration time constant or superexcitability, indicative of internodal and nodal properties, respectively (Bostock et al., 1998; Kiernan et al., 2000). Furthermore, another limitation is the investigated demographic involved individuals without any neurological impairments. Primary users of NMES typically have a neurological or musculoskeletal impairment, and the translation of these results into this population remains unclear.

3.5. Future Directions

Future directions of the present study could further expand on the idea that decreases in axonal excitability contribute to contraction fatigability. One important experiment will be to analyze this phenomenon in a population of individuals with a spinal cord injury (SCI) – a demographic that includes frequent users of NMES. As shown in a rat model, type I muscles demonstrate better accommodation to hyperpolarization compared to type II muscles (Lorenz & Jones, 2014). In individuals with a SCI, muscles undergo a metamorphosis from type I to primarily type II muscles. This suggests that compared to the TA muscle of a neurologically intact individual which is primarily composed of type I fibres, we would expect greater increases in the threshold current in the same muscle in individuals with a SCI.

Another potential experiment is to explore if alternative methods of delivering NMES may reduce the magnitude of decreases in axonal excitability. One such method includes distributing the stimulation among multiple electrodes placed over the muscle belly, or in conjunction with the nerve trunk innervating the muscle. These methods reduce the discharge rate of MUs beneath each stimulating electrode, thereby reducing their respective impulse load. Based on the results of the present study, we would hypothesize that the decrease in MU discharge rates at each site would further reduce changes in excitability. Another alternative form of stimulation incorporates reflexive pathways through the spinal cord to replicate the physiological way MUs are recruited during voluntary contractions. During low-strength contractions, these reflexive pathways preferentially activate small MUs, which has demonstrated increased accommodation to axonal hyperpolarization (Lorenz & Jones, 2014). This leaves reason to believe that generating

contractions through these pathways will reduce changes in axonal excitability thus providing more fatigability-resistant contractions.

3.6. Summary

This thesis focused on contraction fatigability that occurs during NMES-evoked isometric contractions in the TA muscle tested in a population with no neurological impairments. Both decreases in axonal excitability and the force-generating capacity of the muscle were found to contribute to decreases in torque, with the former being the dominant factor overall. At each frequency, neuromuscular transmission was found to be unaffected. A future step of the present study will be to perform these experiments in individuals with a neurological injury such as a SCI, with the hopes of better understanding and minimizing factors contributing to contraction fatigability.

REFERENCES

- Aldrich, T. K., Shander, A., Chaudhry, I., & Nagashima, H. (1986). Fatigue of isolated rat diaphragm: role of impaired neuromuscular transmission. *Journal of Applied Physiology*, *61*(3), 1077–1083.
- Allen, D. G., Lamb, G. D., & Westerblad, H. (2008). Skeletal muscle fatigue: cellular mechanisms. *Physiological Reviews*, *88*(1), 287–332. <http://doi.org/10.1152/physrev.00015.2007>.
- Badier, M., Guillot, C., Danger, C., Tagliarini, F., & Jammes, Y. (1999). M-wave changes after high- and low-frequency electrically induced fatigue in different muscles. *Muscle and Nerve*, *22*, 488–496.
- Bajd, T., Kralj, A., Turk, R., Benko, H., & Segal, J. (1989). Use of functional electrical stimulation in the rehabilitation of patients with incomplete spinal cord injuries. *Journal of Biomedical Engineering*, *11*(2), 96–102.
- Baldi, J. C., Jackson, R. D., Moraille, R., & Mysiw, W. J. (1998). Muscle atrophy is prevented in patients with acute spinal cord injury using functional electrical stimulation. *Spinal Cord*, *36*(7), 463–9.
- Balog, E. M., Thompson, L. V., & Fitts, R. H. (1994). Role of sarcolemma action potentials and excitability in muscle fatigue. *Journal of Applied Physiology*, *76*(5), 2157–2162.
- Barss, T. S., Ainsley, E. N., Claveria-Gonzalez, F. C., Luu, M. J., Miller, D. J., Wiest, M. J., & Collins, D. F. (n.d.). Utilising physiological principles of motor unit recruitment to reduce fatigability of electrically-evoked contractions : A narrative review. *Archives of Physical Medicine and Rehabilitation*.
- Behringer, M., Grutzner, S., Montag, J., Mccourt, M., Ring, M., & Mester, J. (2016). Effects of stimulation frequency, amplitude, and impulse width on muscle fatigue. *Muscle and Nerve*, *53*(4), 608–16. <http://doi.org/10.1002/mus.24893>
- Bergmans, J. (1970). *The physiology of single human nerve fibres*.
- Berkelmans, R. (2008). FES cycling. *Journal of Automatic Control*, *18*(2), 73–76. <http://doi.org/10.2298/JAC0802073B>
- Bertoti, D. B. (2000). Electrical stimulation: a reflection on current clinical practices. *Assist Technol*, *12*(1), 21–32. <http://doi.org/10.1080/10400435.2000.10132007>
- Bezaniilla, F., Caputo, C., Gonzalez-Serratos, H., & Venosa, R. A. (1972). Sodium dependence of the inward spread of activation in isolated twitch muscle fibres of the frog. *Journal of Physiology*, *223*(2), 507–523.
- Bickel, C. S., Gregory, C. M., & Dean, J. C. (2011). Motor unit recruitment during neuromuscular electrical stimulation: A critical appraisal. *European Journal of Applied Physiology*, *111*(10), 2399–2407. <http://doi.org/10.1007/s00421-011-2128-4>

- Bigland-Ritchie, B., Jones, D. A., & Woods, J. J. (1979). Excitation frequency and muscle fatigue: electrical responses during human voluntary and stimulated contractions. *Experimental Neurology*, *64*(2), 414–427.
- Bigland-Ritchie, B., Kukulka, C. G., Lippold, O. C. J., & Woods, J. J. (1982). The absence of neuromuscular transmission failure in sustained maximal voluntary contractions. *Journal of Physiology*, *330*, 265–278.
- Bigland-Ritchie, B. R., Furbush, F. H., Gandevia, S. C., & Thomas, C. K. (1992). Voluntary discharge frequencies of human motoneurons at different muscle lengths. *Muscle and Nerve*, *15*, 130–137. <http://doi.org/10.1002/mus.880150203>
- Binder-Macleod, S. A., & Russ, D. W. (1999). Effects of activation frequency and force on low-frequency fatigue in human skeletal muscle. *Journal of Applied Physiology*, *86*(4), 1337–1346.
- Bostock, H., Cikurel, K., & Burke, D. (1998). Threshold tracking techniques in the study of human peripheral nerve. *Muscle and Nerve*, *21*, 137–158.
- Bostock, H., & Grafe, P. (1985). Activity-dependent excitability changes in normal and demyelinated rat spinal root axons. *Journal of Physiology*, *365*, 239–257.
- Bostock, H., & Rothwell, J. C. (1997). Latent addition in motor and sensory fibres of human peripheral nerve. *Journal of Physiology*, *498*(1), 277–94.
- Botter, A., Oprandi, G., Lanfranco, F., Allasia, S., Maffiuletti, N. A., & Minetto, M. A. (2011). Atlas of the muscle motor points for the lower limb: implications for electrical stimulation procedures and electrode positioning. *European Journal of Applied Physiology*, *111*(10), 2461–2471.
- Broderick, B. J., Kennedy, C., Breen, P. P., Kearns, S. R., & Ólaighin, G. (2011). Patient tolerance of neuromuscular electrical stimulation (NMES) in the presence of orthopaedic implants. *Medical Engineering and Physics*, *33*(1), 56–61. <http://doi.org/10.1016/j.medengphy.2010.09.003>
- Bruton, J. D., Place, N., Yamada, T., Silva, J. P., Andrade, F. H., Dahlstedt, A. J., ... Westerblad, H. (2008). Reactive oxygen species and fatigue-induced prolonged low-frequency force depression in skeletal muscle fibres of rats, mice and SOD2 overexpressing mice. *Journal of Physiology*, *586*(1), 175–184. <http://doi.org/10.1113/jphysiol.2007.147470>
- Burke, D., Kiernan, M. C., & Bostock, H. (2001). Excitability of human axons. *Clinical Neurophysiology*, *112*(9), 1575–1585. [http://doi.org/10.1016/S1388-2457\(01\)00595-8](http://doi.org/10.1016/S1388-2457(01)00595-8)
- Cambridge, N. A. (1977). Electrical apparatus used in medicine before 1900. *Proceedings of the Royal Society of Medicine*, *70*(9), 635–41. <http://doi.org/10.1177/003591577707000909>
- Chiou-Tan, F. Y., Tim, R. W., Gilchrist, J. M., Weber, C. F., Wilson, J. R., Benstead, T. J., ... Ryan, K. S. (2001). Literature review of the usefulness of repetitive nerve stimulation and single fiber EMG in the electrodiagnostic evaluation of patients with suspected myasthenia gravis or Lambert-Eaton myasthenic syndrome. *Muscle and Nerve*, *24*(9), 1239–1247.

<http://doi.org/10.1002/mus.1140>

- Choi, J.-S., Hudmon, A., Waxman, S. G., & Dib-Hajj, S. D. (2006). Calmodulin Regulates Current Density and Frequency-Dependent Inhibition of Sodium Channel Nav1.8 in DRG Neurons. *Journal of Neurophysiology*, *96*(1), 97–108. <http://doi.org/10.1152/jn.00854.2005>
- Clausen, T. (1996). The Na⁺, K⁺ pump in skeletal muscle: quantification, regulation and functional significance. *Acta Physiologica Scandinavica*, *156*, 227–235. <http://doi.org/10.1046/j.1365-201X.1996.209000.x>
- Collins, D. F. (2007). Central contributions to contractions evoked by tetanic neuromuscular electrical stimulation. *Exercise and Sport Sciences Reviews*, *35*(3), 102–109.
- Connelly, D. M., Rice, C. L., Roos, M. R., & Vandervoort, A. A. (1999). Motor unit firing rates and contractile properties in tibialis anterior of young and old men. *Journal of Applied Physiology*, *87*(2), 843–852.
- Cooper, R. G., Edwards, R. H. T., Gibson, H., & Stokes, M. J. (1988). Human muscle fatigue: frequency dependence of excitation and force generation. *Journal of Physiology*, *397*, 585–599.
- Costa, J., Evangelista, T., Conceição, I., & de Carvalho, M. (2004). Repetitive nerve stimulation in myasthenia gravis--relative sensitivity of different muscles. *Clinical Neurophysiology*, *115*(12), 2776–2782. <http://doi.org/10.1016/j.clinph.2004.05.024>
- Cramer, R. M., Weston, A., Climstein, M., Davis, G. M., & Sutton, J. R. (2002). Effects of electrical stimulation-induced leg training on skeletal muscle adaptability in spinal cord injury. *Scandinavian Journal of Medicine & Science in Sports*, *12*(5), 316–322. <http://doi.org/10.1034/j.1600-0838.2002.20106.x>
- Cupido, C. M., Galea, V., & McComas, A. J. (1996). Potentiation and depression of the M wave in human biceps brachii. *Journal of Physiology*, *491*(2), 541–550.
- Dali, C., Hansen, F. J., Pedersen, S. A., Skov, L., Hilden, J., Bjornskov, I., ... Lyskjaer, U. (2002). Threshold Electrical Stimulation (TES) in Ambulant Children with CP: a Randomized Double - Blind Placebo - Controlled Clinical Trial. *Developmental Medicine and Child Neurology*, *44*, 364–369. <http://doi.org/10.1097/00004703-200302000-00022>
- de Kroon, J. R., IJzerman, M. J., Chae, J., Lankhorst, G. J., & Zilvold, G. (2005). Relation between stimulation characteristics and clinical outcome in studies using electrical stimulation to improve motor control of the upper extremity in stroke. *Journal of Rehabilitation Medicine*, *37*(2), 65–74. <http://doi.org/10.1080/16501970410024190>
- De Luca, C. J., & Contessa, P. (2012). Hierarchical control of motor units in voluntary contractions. *Journal of Neurophysiology*, *107*(1), 178–195. <http://doi.org/10.1152/jn.00961.2010>
- De Weer, P., & Geduldig, D. (1973). Electrogenic sodium pump in squid giant axon. *Science*, *179*(80), 1326–1328.

- Desaulniers, P., Lavoie, P. A., & Gardiner, P. F. (2002). Incomplete recovery of endplate potential amplitude while intermittently activating rat soleus neuromuscular junctions in situ. *Muscle and Nerve*, 26(6), 810–816. <http://doi.org/10.1002/mus.10275>
- Desmedt, J. E., & Godaux, E. (1977). Ballistic contractions in man: characteristic recruitment pattern of single motor units of the tibialis anterior muscle. *Journal of Physiology*, 264, 673–693. <http://doi.org/10.1113/jphysiol.1977.sp011689>
- Duffell, L. D., Donaldson, N. D. N., Perkins, T. A., Rushton, D. N., Hunt, K. J., Kakebeeke, T. H., & Newham, D. J. (2008). Long-term intensive electrically stimulated cycling by spinal cord-injured people: effect on muscle properties and their relation to power output. *Muscle and Nerve*, 38(4), 1304–11. <http://doi.org/10.1002/mus.21060>
- Dulhunty, A. F. (2006). Excitation-contraction coupling from the 1950s into the new millennium. *Clinical and Experimental Pharmacology and Physiology*, 33(9), 763–772. <http://doi.org/10.1111/j.1440-1681.2006.04441.x>
- Edwards, R. H. (1984). New techniques for studying human muscle function, metabolism, and fatigue. *Muscle and Nerve*, 7(8), 599–609. <http://doi.org/10.1002/mus.880070802>
- Edwards, R. H., Hill, D. K., Jones, D. A., & Merton, P. A. (1977). Fatigue of long duration in human skeletal muscle after exercise. *Journal of Physiology*, 272(3), 769–778. <http://doi.org/10.1113/jphysiol.1977.sp012072>
- Edwards, R. H., Young, A., Hosking, G. P., & Jones, D. A. (1977). Human skeletal muscle function: description of tests and normal values. *Clinical Science and Molecular Medicine*, 52(3), 283–290.
- Endo, M. (1975). Mechanism of action of caffeine on the sarcoplasmic reticulum of skeletal muscle. *Proceedings of the Japan Academy*, 51(6), 479–484.
- Enoka, R. M., & Duchateau, J. (2008). Muscle fatigue: what, why and how it influences muscle function. *Journal of Physiology*, 586(1), 11–23. <http://doi.org/10.1113/jphysiol.2007.139477>
- Enoka, R. M., & Duchateau, J. (2017). Rate coding and the control of muscle force. *Cold Spring Harb Perspect Med*. <http://doi.org/10.1101/cshperspect.a029702>
- Ermilov, L. G., Mantilla, C. B., Rowley, K. L., & Sieck, G. C. (2007). Safety factor for neuromuscular transmission at type-identified diaphragm fibers. *Muscle and Nerve*, 35(6), 800–803. <http://doi.org/10.1002/mus.20751>
- Fehlings, D. L., Kirsch, S., McComas, A., Chipman, M., & Campbell, K. (2002). Evaluation of therapeutic electrical stimulation to improve muscle strength and function in children with types II/III spinal muscular atrophy. *Developmental Medicine and Child Neurology*, 44(11), 741–744. <http://doi.org/10.1017/S0012162201002869>
- Fitts, R. H. (1994). Cellular mechanisms of muscle fatigue. *Physiological Reviews*, 74(1), 49–94.
- Frigon, A., Carroll, T. J., Jones, K. E., Zehr, E. P., & Collins, D. F. (2007). Ankle position and

- voluntary contraction alter maximal M waves in soleus and tibialis anterior. *Muscle and Nerve*, 35(6), 756–766. <http://doi.org/10.1002/mus.20747>
- Frotzler, A., Coupaud, S., Perret, C., Kakebeeke, T. H., Hunt, K. J., Donaldson, N. D. N., & Eser, P. (2008). High-volume FES-cycling partially reverses bone loss in people with chronic spinal cord injury. *Bone*, 43, 169–176. <http://doi.org/10.1016/j.bone.2008.03.004>
- Fuglevand, A. J., Zackowski, K. M., Huey, K. A., & Enoka, R. M. (1993). Impairment of neuromuscular propagation during human fatiguing contractions at submaximal forces. *Journal of Physiology*, 460, 549–572.
- Gibson, H., Cooper, R. G., Stokes, M. J., & Edwards, R. H. (1988). Mechanisms resisting fatigue in isometrically contracting human skeletal muscle. *Quarterly Journal of Experimental Physiology*, 73(6), 903–14. <http://doi.org/10.1113/expphysiol.1988.sp003225>
- Gorgey, A. S., Black, C. D., Elder, C. P., & Dudley, G. A. (2009). Effects of electrical stimulation parameters on fatigue in skeletal muscle. *Journal of Orthopaedic & Sports Physical Therapy*, 39(9), 684–692. <http://doi.org/10.2519/jospt.2009.3045>
- Hamzaid, N. A., & Davis, G. M. (2009). Health and fitness benefits of functional electrical stimulation-evoked leg exercise for spinal cord-injured individuals. *Topics in Spinal Cord Injury Rehabilitation*, 14(4), 88–121. <http://doi.org/10.1310/sci1404-88>
- Heidland, A., Fazeli, G., Klassen, A., Sebekova, K., Hennemann, H., Bahner, U., & Di Iorio, B. (2013). Neuromuscular electrostimulation techniques: historical aspects and current possibilities in treatment of pain and muscle wasting. *Clinical Nephrology*, 79(13), 12–23. <http://doi.org/10.5414/CNX77S106>
- Henneman, E., Somjen, G., & Carpenter, D. O. (1965). Excitability and inhibibility of motoneurons of different sizes. *Journal of Neurophysiology*, 28(3), 599–620.
- Hermansen, L. (1981). Effect of metabolic changes on force generation in skeletal muscle during maximal exercise. *Ciba Foundation Symposium*, 82, 75–88.
- Hicks, A., & McComas, A. J. (1989). Increased sodium pump activity following repetitive stimulation of rat soleus muscles. *Journal of Physiology*, 414(1989), 337–49. <http://doi.org/10.1113/jphysiol.1989.sp017691>
- Hille, B. (2001). *Ion channels of excitable membranes*. Sinauer Associates, Inc. http://doi.org/10.1007/3-540-29623-9_5640
- Howells, J., Trevillion, L., Bostock, H., & Burke, D. (2012). The voltage dependence of I_h in human myelinated axons. *Journal of Physiology*, 590(7), 1625–1640. <http://doi.org/10.1113/jphysiol.2011.225573>
- Jaeger, R. J., Yarkony, G. M., & Smith, R. M. (1989). Standing the spinal cord injured patient by electrical stimulation: refinement of a protocol for clinical use. *IEEE Transactions on Biomedical Engineering*, 36(7), 720–728. <http://doi.org/10.1109/10.32104>
- Johnson, M. A., Polgar, J., Weightman, D., & Appleton, D. (1973). Data on the distribution of

- fibre types in thirty-six human muscles. An autopsy study. *Journal of the Neurological Sciences*, 18(1), 111–129. [http://doi.org/10.1016/0022-510X\(73\)90023-3](http://doi.org/10.1016/0022-510X(73)90023-3)
- Jones, D. A. (1981). Muscle fatigue due to changes beyond the neuromuscular junction. *Ciba Foundation Symposium*, 82, 178–96.
- Jones, D. A. (1996). High- and low-frequency fatigue revisited. *Acta Physiologica Scandinavica*, 156, 265–270.
- Jones, D. A., Bigland-Ritchie, B., & Edwards, R. H. T. (1979). Excitation frequency and muscle fatigue: mechanical responses during voluntary and stimulated contractions. *Experimental Neurology*, 64(2), 414–427. [http://doi.org/10.1016/0014-4886\(79\)90280-2](http://doi.org/10.1016/0014-4886(79)90280-2)
- Jones, D. A., Howell, S., Roussos, C., & Edwards, R. H. (1982). Low-frequency fatigue in isolated skeletal muscles and the effects of methylxanthines. *Clinical Science*, 63(2), 161–167. <http://doi.org/10.1042/CS0630161>
- Juel, C. (1986). Potassium and sodium shifts during in vitro isometric muscle contraction, and the time course of the ion-gradient recovery. *Pflugers Archiv European Journal of Physiology*, 406(5), 458–463. <http://doi.org/10.1007/BF00583367>
- Keenan, K. G., Farina, D., Merletti, R., & Enoka, R. M. (2006). Influence of motor unit properties on the size of the simulated evoked surface EMG potential. *Experimental Brain Research*, 169(1), 37–49. <http://doi.org/10.1007/s00221-005-0126-7>
- Keeton, R. B., & Binder-Macleod, S. A. (2006). Low-frequency fatigue. *Physical Therapy*, 86, 1146–1150.
- Kiernan, M. C., Burke, D., Andersen, K. V., & Bostock, H. (2000). Multiple measures of axonal excitability: a new approach in clinical testing. *Muscle and Nerve*, 23, 399–409. [http://doi.org/10.1002/\(SICI\)1097-4598\(200003\)23:3<399::AID-MUS12>3.0.CO;2-G](http://doi.org/10.1002/(SICI)1097-4598(200003)23:3<399::AID-MUS12>3.0.CO;2-G) [pii]
- Kiernan, M. C., Lin, C. S.-Y., & Burke, D. (2004). Differences in activity-dependent hyperpolarization in human sensory and motor axons. *Journal of Physiology*, 558(1), 341–349. <http://doi.org/10.1113/jphysiol.2004.063966>
- Kiernan, M. C., & Lin, C. S. Y. (2012). *Nerve excitability: a clinical translation*. Aminoff's *Electrodiagnosis in Clinical Neurology* (6th ed.). Elsevier Inc. <http://doi.org/10.1016/B978-1-4557-0308-1.00015-7>
- Klein, C. S., Zhou, P., & Marciniak, C. (2015). Excitability properties of motor axons in adults with cerebral palsy. *Frontiers in Human Neuroscience*, 9(June), 329. <http://doi.org/10.3389/fnhum.2015.00329>
- Kluger, B. M., Krupp, L. B., & Enoka, R. M. (2013). Fatigue and fatigability in neurologic illnesses: proposal for a unified taxonomy. *Neurology*, 80(4), 409–416. <http://doi.org/10.1212/WNL.0b013e31827f07be>
- Knutson, J. S., Fu, M. J., Sheffler, L. E., & Chae, J. (2015). Neuromuscular electrical stimulation for motor restoration in hemiplegia. *Physical Medicine and Rehabilitation Clinics of North*

America, 26, 729–745. <http://doi.org/10.1016/j.pmr.2015.06.002>

- Kralj, A. R., & Bajd, T. (1989). *Functional electrical stimulation : standing and walking after spinal cord injury*. CRC Press.
- Krishnan, A. V., Lin, C. S.-Y., & Kiernan, M. C. (2008). Activity-dependent excitability changes suggest Na⁺/K⁺ pump dysfunction in diabetic neuropathy. *Brain*, 131(5), 1209–1216. <http://doi.org/10.1093/brain/awn052>
- Krishnan, A. V., Lin, C. S.-Y., Park, S. B., & Kiernan, M. C. (2009). Axonal ion channels from bench to bedside: A translational neuroscience perspective. *Progress in Neurobiology*, 89(3), 288–313. <http://doi.org/10.1016/j.pneurobio.2009.08.002>
- Krnjevic, K., & Miledi, R. (1958). Failure of neuromuscular propagation in rats. *Journal of Physiology*, 140(3), 440–461. <http://doi.org/10.1113/jphysiol.1959.sp006321>
- Krnjevic, K., & Miledi, R. (1959). Presynaptic failure of neuromuscular propagation in rats. *Journal of Physiology*, 149(1), 1–22. <http://doi.org/10.1113/jphysiol.1959.sp006321>
- Kuwabara, S., Cappelen-Smith, C., Lin, C. S.-Y., Mogyoros, I., & Burke, D. (2002). Effects of voluntary activity on the excitability of motor axons in the peroneal nerve. *Muscle and Nerve*, 25(2), 176–184. <http://doi.org/10.1002/mus.10030>
- Kuwabara, S., Cappelen-Smith, C., Lin, C. S. Y., Mogyoros, I., Bostock, H., & Burke, D. (2000). Excitability properties of median and peroneal motor axons. *Muscle and Nerve*, 23(9), 1365–1373. [http://doi.org/10.1002/1097-4598\(200009\)23:9<1365::AID-MUS7>3.0.CO;2-1](http://doi.org/10.1002/1097-4598(200009)23:9<1365::AID-MUS7>3.0.CO;2-1)
- Lamb, G. D. (2009). Mechanisms of excitation-contraction uncoupling relevant to activity-induced muscle fatigue. *Applied Physiology, Nutrition, and Metabolism*, 34(3), 368–372. <http://doi.org/10.1139/H09-032>
- Liberson, W. T., Holmquest, H. J., Scot, D., & Dow, M. (1961). Functional electrotherapy: stimulation of the peroneal nerve synchronized with the swing phase of the gait of hemiplegic patients. *Archives of Physical Medicine and Rehabilitation*, 42, 101–5.
- Liik, M., & Punga, A. R. (2016). Repetitive nerve stimulation often fails to detect abnormal decrement in acute severe generalized Myasthenia Gravis. *Clinical Neurophysiology*, 127(11), 3480–3484. <http://doi.org/10.1016/j.clinph.2016.09.012>
- Lin, C. S. Y., Macefield, V. G., Elam, M., Wallin, B. G., Engel, S., & Kiernan, M. C. (2007). Axonal changes in spinal cord injured patients distal to the site of injury. *Brain*, 130(4), 985–994. <http://doi.org/10.1093/brain/awl339>
- Lorenz, C., & Jones, K. E. (2014). IH activity is increased in populations of slow versus fast motor axons of the rat. *Frontiers in Human Neuroscience*, 8(September), 1–9. <http://doi.org/10.3389/fnhum.2014.00766>
- Lou, J. W. W. H., Bergquist, A. J., Aldayel, A., Czitron, J., & Collins, D. F. (2017). Interleaved neuromuscular electrical stimulation reduces muscle fatigue. *Muscle and Nerve*, 55(2), 179–189. <http://doi.org/10.1002/mus.25224>

- Lüttgau, H. (1965). The effect of metabolic inhibitors on the fatigue of the action potential in single muscle fibres. *Journal of Physiology*, *178*, 45–67.
- Macdonald, A. J. R. (1993). A brief review of the history of electrotherapy and its union with acupuncture. *Acupuncture in Medicine*, *11*(2), 66–75.
- Maffiuletti, N. A. (2010). Physiological and methodological considerations for the use of neuromuscular electrical stimulation. *European Journal of Applied Physiology*, *110*(2), 223–234. <http://doi.org/10.1007/s00421-010-1502-y>
- Maffiuletti, N. A., Roig, M., Karatzanos, E., & Nanas, S. (2013). Neuromuscular electrical stimulation for preventing skeletal-muscle weakness and wasting in critically ill patients: a systematic review. *BMC Medicine*, *11*(1), 137. <http://doi.org/10.1186/1741-7015-11-137>
- Martin, A., Grospretre, S., Vilmen, C., Guye, M., Mattei, J. P., Le Fur, Y., ... Gondin, J. (2016). The etiology of muscle fatigue differs between two electrical stimulation protocols. *Medicine and Science in Sports and Exercise*, *48*(8), 1474–1484. <http://doi.org/10.1249/MSS.0000000000000930>
- Martin, R., Sadowsky, C., Obst, K., Meyer, B., & McDonald, J. (2012). Functional Electrical Stimulation in Spinal Cord Injury: From Theory to Practice. *Topics in Spinal Cord Injury Rehabilitation*, *18*(1), 28–33. <http://doi.org/10.1310/sci1801-28>
- Matkowski, B., Lepers, R., & Martin, A. (2015). Torque decrease during submaximal evoked contractions of the quadriceps muscle is linked not only to muscle fatigue. *Journal of Applied Physiology*, *118*(9), 1136–1144. <http://doi.org/10.1152/jappphysiol.00553.2014>
- Mckenna, M. J., Bangsbo, J., & Renaud, J.-M. (2008). Muscle K⁺, Na⁺, and Cl⁻ disturbances and Na⁺-K⁺ pump inactivation: implications for fatigue. *Journal of Applied Physiology*, *104*, 288–295. <http://doi.org/10.1152/jappphysiol.01037.2007>.
- Merletti, R., Lo Conte, L. R., & Orizio, C. (1991). Indices of muscle fatigue. *Journal of Electromyography and Kinesiology*, *1*(1), 20–33. [http://doi.org/10.1016/1050-6411\(91\)90023-X](http://doi.org/10.1016/1050-6411(91)90023-X)
- Merton, P. A. (1954). Voluntary strength and fatigue. *Journal of Physiology*, *123*, 553–564.
- Merton, P. A., Hill, D. K., & Morton, H. B. (1981). Indirect and direct stimulation of fatigued human muscle. *Ciba Foundation Symposium*, *82*, 120–9.
- Milner-Brown, H. S., & Miller, R. G. (1986). Muscle membrane excitation and impulse propagation velocity are reduced during muscle fatigue. *Muscle and Nerve*, *9*(4), 367–374. <http://doi.org/10.1002/mus.880090415>
- Milner-Brown, H. S., Stein, R. B., & Yemm, R. (1973). The orderly recruitment of human motor units during voluntary isometric contractions. *Journal of Physiology*, *230*(2), 359–70. <http://doi.org/10.1113/jphysiol.1973.sp010192>
- Mortimer, J. T. (2011). Motor Prostheses. In *Comprehensive Physiology*. Hoboken, NJ, USA: John Wiley & Sons, Inc. <http://doi.org/10.1002/cphy.cp010205>

- Nagaoka, R., Yamashita, S., Mizuno, M., & Akaike, N. (1994). Intracellular Na⁺ and K⁺ shifts induced by contractile activities of rat skeletal muscles. *Comparative Biochemistry and Physiology*, *109*(4), 957–965. [http://doi.org/10.1016/0300-9629\(94\)90244-5](http://doi.org/10.1016/0300-9629(94)90244-5)
- Nodera, H., & Kaji, R. (2006). Nerve excitability testing and its clinical application to neuromuscular diseases. *Clinical Neurophysiology*, *117*(9), 1902–16. <http://doi.org/10.1016/j.clinph.2006.01.018>
- Ozdemir, C., & Young, R. R. (1976). The results to be expected from electrical testing in the diagnosis of Myasthenia Gravis. *Annals of the New York Academy of Sciences*, *274*, 203–22.
- Pagala, M. K. D., Namba, T., & Grob, D. (1984). Failure of neuromuscular transmission and contractility during muscle fatigue. *Muscle and Nerve*, *7*(6), 454–464. <http://doi.org/10.1002/mus.880070607>
- Panizza, M., Nilsson, J., Roth, B. J., Grill, S. E., Demirci, M., & Hallett, M. (1998). Differences between the time constant of sensory and motor peripheral nerve fibers: further studies and considerations. *Muscle and Nerve*, *21*(1), 48–54.
- Papaiordanidou, M., Billot, M., Varray, A., & Martin, A. (2014). Neuromuscular Fatigue Is Not Different between Constant and Variable Frequency Stimulation. *PLoS ONE*, *9*(1), e84740. <http://doi.org/10.1371/journal.pone.0084740>
- Papaiordanidou, M., Stevenot, J.-D., Mustacchi, V., Vanoncini, M., & Martin, A. (2014). Electrically induced torque decrease reflects more than muscle fatigue. *Muscle and Nerve*, *50*(4), 604–607. <http://doi.org/10.1002/mus.24276>
- Pape, K. E. (1997). Therapeutic electrical stimulation (TES) for the treatment of disuse muscle atrophy in cerebral palsy. *Pediatric Physical Therapy*, *9*, 110–112.
- Pape, K., Kirsch, S., Galil, A., Boulton, J., White, A., & Chipman, M. (1993). Neuromuscular approach to the motor deficits of cerebral palsy: a pilot study. *Journal of Pediatric Orthopaedics*, *13*(5), 628–633.
- Parent, A. (2004). Giovanni Aldini: from animal electricity to human brain stimulation. *Canadian Journal of Neurological Sciences*, *31*(4), 576–584. <http://doi.org/10.1017/S0317167100003851>
- Peckham, P. H., & Knutson, J. S. (2005). Functional electrical stimulation for neuromuscular applications*. *Annual Review of Biomedical Engineering*, *7*(1), 327–360. <http://doi.org/10.1146/annurev.bioeng.6.040803.140103>
- Place, N., Yamada, T., Bruton, J. D., & Westerblad, H. (2010). Muscle fatigue: from observations in humans to underlying mechanisms studied in intact single muscle fibres. *European Journal of Applied Physiology*, *110*(1), 1–15. <http://doi.org/10.1007/s00421-010-1480-0>
- Popović, L. Z., & Malešević, N. M. (2009). Muscle fatigue of quadriceps in paraplegics: Comparison between single vs. multi-pad electrode surface stimulation. In *Proceedings of*

the 31st Annual International Conference of the IEEE Engineering in Medicine and Biology Society: Engineering the Future of Biomedicine, EMBC 2009 (pp. 6785–6788).
<http://doi.org/10.1109/IEMBS.2009.5333983>

- Reid, B., Slater, C. R., & Bewick, G. S. (1999). Synaptic vesicle dynamics in rat fast and slow motor nerve terminals. *Journal of Neuroscience*, *19*(7), 2511–2521.
- Rich, M. M. (2006). The control of neuromuscular transmission in health and disease. *The Neuroscientist*, *12*(2), 134–142. <http://doi.org/10.1177/1073858405281898>
- Roussos, C., & Aubier, M. (1981). Neural drive and electromechanical alterations in the fatiguing diaphragm. *Ciba Foundation Symposium*, *82*, 213–33.
- Sacco, P., McIntyre, D. B., & Jones, D. a. (1994). Effects of length and stimulation frequency on fatigue of the human tibialis anterior muscle. *Journal of Applied Physiology*, *77*(3), 1148–1154.
- Schechter, D. C. (1971). Origins of electrotherapy II. *New York State Journal of Medicine*, *71*(10), 1114–24.
- Sheffler, L. R., & Chae, J. (2007). Neuromuscular electrical stimulation in neurorehabilitation. *Muscle and Nerve*, *35*(5), 562–590. <http://doi.org/10.1002/mus.20758>
- Sieck, G. C., & Prakash, Y. S. (1995). Fatigue at the neuromuscular junction. Branch point vs. presynaptic vs. postsynaptic mechanisms. *Advances in Experimental Medicine and Biology*, *384*, 83–100.
- Sommerfelt, K., Markestad, T., Berg, K., & Saetesdal, I. (2001). Therapeutic electrical stimulation in cerebral palsy: a randomized, controlled, crossover trial. *Developmental Medicine & Child Neurology*, *43*(9), 609–613. <http://doi.org/10.1111/j.1469-8749.2001.tb00243.x>
- Stephens, J. A., & Taylor, A. (1972). Fatigue of maintained voluntary muscle contraction in man. *Journal of Physiology*, *220*(1), 1–18. <http://doi.org/10.1113/jphysiol.1972.sp009691>
- Stephenson, D. G., Lamb, G. D., Stephenson, G. M. M., & Fryer, M. W. (1995). Mechanisms excitation-contraction coupling relevant to skeletal muscle fatigue. *Advances in Experimental Medicine and Biology*, *384*, 45–56.
- Stillings, D. (1983). Mediterranean origins of electrotherapy. *Journal of Bioelectricity*, *2*(2–3), 181–186. <http://doi.org/10.3109/15368378309009849>
- Tasaki, I. (1953). *Nervous transmission* (First Edit). Charles C. Thomas, Springfield, Illinois.
- Taylor, J. A., Picard, G., & Widrick, J. J. (2011). Aerobic capacity with hybrid FES rowing in spinal cord injury: comparison with arms-only exercise and preliminary findings with regular training. *Physical Medicine and Rehabilitation*, *3*(9), 817–824.
<http://doi.org/10.1016/j.pmrj.2011.03.020>
- Thesleff, S. (1959). Motor end-plate “desensitization” by repetitive nerve stimuli. *Journal of*

Physiology, 148, 659–664.

- Thomas, C. K., Griffin, L., Godfrey, S., Ribot-Ciscar, E., & Butler, J. E. (2003). Fatigue of paralyzed and control thenar muscles induced by variable or constant frequency stimulation. *Journal of Neurophysiology*, 89(4), 2055–64. <http://doi.org/10.1152/jn.01002.2002>
- Thomas, C. K., Woods, J. J., & Bigland-Ritchie, B. (1989). Impulse propagation and muscle activation in long maximal voluntary contractions. *Journal of Applied Physiology*, 67(5), 1835–1842.
- Tucker, K. J., & Turker, K. S. (2007). Triceps surae stretch and voluntary contraction alters maximal M-wave magnitude. *Journal of Electromyography and Kinesiology*, 17(2), 203–211. <http://doi.org/10.1016/j.jelekin.2005.12.006>
- Vagg, R., Mogyoros, I., Kiernan, M. C., & Burke, D. (1998). Activity-dependent hyperpolarization of human motor axons produced by natural activity. *Journal of Physiology*, 507(3), 919–925. <http://doi.org/10.1111/j.1469-7793.1998.919bs.x>
- Veale, J. L., Mark, R. F., & Rees, S. (1973). Differential sensitivity of motor and sensory fibres in human ulnar nerve. *Journal of Neurology, Neurosurgery and Psychiatry*, 36(1), 75–86. <http://doi.org/10.1136/jnnp.36.1.75>
- Vucic, S., Krishnan, A. V., & Kiernan, M. C. (2007). Fatigue and activity dependent changes in axonal excitability in amyotrophic lateral sclerosis. *Journal of Neurology, Neurosurgery and Psychiatry*, 78(11), 1202–1208. <http://doi.org/10.1136/jnnp.2006.112078>
- Waxman, S. G., & Ritchie, J. M. (1985). Organization of ion channels in the myelinated nerve fiber. *Science*, 228(4707), 1502–1507. <http://doi.org/10.1126/science.2409596>
- Weigl, P., Bostock, H., Franz, P., Martius, P., Müller, W., & Grafe, P. (1989). Threshold tracking provides a rapid indication of ischaemic resistance in motor axons of diabetic subjects. *Electroencephalography and Clinical Neurophysiology*, 73, 369–371. [http://doi.org/10.1016/0013-4694\(89\)90115-6](http://doi.org/10.1016/0013-4694(89)90115-6)
- Westerblad, H., Allen, D. G., & Lännergren, J. (2002). Muscle fatigue : lactic acid or inorganic phosphate the major cause? *News in Physiological Science*, 17(February), 17–21.
- Westerblad, H., Duty, S., & Allen, D. G. (1993). Intracellular calcium concentration during low-frequency fatigue in isolated single fibers of mouse skeletal muscle. *Journal of Applied Physiology*, 75(1), 382–388.
- Westerblad, H., Lee, J. A., Lännergren, J., & Allen, D. G. (1991). Cellular mechanisms of fatigue in skeletal muscle. *American Journal of Physiology*, 261(30), C195–C209.
- Wheeler, G. D., Andrews, B., Lederer, R., Davoodi, R., Natho, K., Weiss, C., ... Steadward, R. D. (2002). Functional electric stimulation-assisted rowing: increasing cardiovascular fitness through functional electric stimulation rowing training in persons with spinal cord injury. *Archives of Physical Medicine and Rehabilitation*, 83(8), 1093–1099. <http://doi.org/10.1053/apmr.2002.33656>

- Wood, S. J., & Slater, C. R. (2001). *Safety factor at the neuromuscular junction*. *Progress in Neurobiology* (Vol. 64). [http://doi.org/10.1016/S0301-0082\(00\)00055-1](http://doi.org/10.1016/S0301-0082(00)00055-1)
- Yan, T., Hui-Chan, C. W. Y., & Li, L. S. W. (2005). Functional electrical stimulation improves motor recovery of the lower extremity and walking ability of subjects with first acute stroke. *Stroke*, *36*, 80–85. <http://doi.org/10.1161/01.STR.0000149623.24906.63>
- Yarkony, G. M., Roth, E. J., Cybulski, G. R., & Jaeger, R. J. (1992). Neuromuscular stimulation in spinal cord injury II: prevention of secondary complications. *Archives of Physical Medicine and Rehabilitation*, *73*(2), 195–200. [http://doi.org/0003-9993\(92\)90101-2](http://doi.org/0003-9993(92)90101-2) [pii]
- Zivković, S. A., & Shipe, C. (2005). Use of repetitive nerve stimulation in the evaluation of neuromuscular junction disorders. *American Journal of Electroneurodiagnostic Technology*, *45*(4), 248–61. <http://doi.org/10.1080/1086508X.2005.11079542>